Table 2. PCR primers used in this study

Primer		Forward	Reverse	Positions*
Hoxb8 proximal	1	aacaggagacagagaaactggtac	actgtttgctttgctgctgtttag	1-516
	2	gggtataaatttctgaaggttaag	agggatgagaagggccgaggg	446-1006
	3	tatgactacctcgttgtttg	caaagactgatgtgggggagt	4292-4565
	4	ggtgtttttccgtgactcccccac	tagaacagcgaagcctgcaaaagt	4531-5091
	5	gccgcggctgccatgcaggcttag	cacggcgcacgggttctgctggta	5045-5568
	6	ttctacggctacgaccctctgcag	cttgagggcgcatccaggg	5593-5764
	7	ccctggatgcgccctcaag	tctccacagcccccataaaac	5746-6083
	8	actgttttatgggggctgtggaga	tctctggtaactagaaccag	6060-6315
	9	tggagctggagaaggagttccta	cagaagctattacgagatactacc	6592-7041
	10	ctccttcccttctcttgggggtcc	caatgctcacagcgcgcatgc	7061-7529
	11	ttagcatgcgcgctgtgagcattg	cactagccaccagcctgggta	7560-8032
	12	cgctcttgggaagagatctaccca	cccaagaggaggcgagcctgg	7994-8584
	13	aggccaggctcgcctcctcttggg	agtcggggacgttttagtgtc	8561-9085
	14	tcacgtggtcagaagagg	ctgagcttcgcatccaggggta	8978-9505
	15	tacccctggatgcgaagctcag	ctagggcctgagagcactgagc	9484-9706
	16	gctcagtgctctcaggccctag	acacccagaactgagctctc	9685-9927
	17	gagagctcagttctgggtgt	accactctttgactctgtgt	9908-10134
	18	acacagagtcaaagagtggt	gtcatctttctggagtgata	10115-10323
	19	tatcactccagaaagatgac	atgagtataggagtctct	10304-10527
	20	agagactcctatactcat	tctgagaactcccagcata	10501-10792
	21	tatgctgggagttctcaga	ctgacagaacttggctctgatg	10774-10985
	22	catcagagccaagttctgtcag	ctgtcatcagtcactctct	10964-11218
	23	agagagtgactgatgacag	agccatcctcctgattcag	11220-11408
	24	ctgcacctagtagtg	tgtaggtctggcggcctcgcttt	11581-11787
	25	ttgtaagccctctttgaagct	taacataaccctcctggcaggccg	12309-12829
Hoxb8 distal	D1	ggtagtagctttctgatggt	aggatgcaaactccattata	
	D2	accatcagaaagctactacc	aacgaatttattgagaattc	
Hoxb3		atgcagaaagccacctacta	ttggacgtttgcctcgactc	
Hoxb6		atgagttcctatttcgtgaa	accagccggcggcggctacg	
Hoxb8		atgagctcttatttcgtcaa	gcttgcagtctgcgtactgc	
Hoxb9		atgtccatttctgggacgct	tggtagacagacggcaggct	
Hoxa4		agctccagccctggcttcgc	cgtgatggatgcygctagcc	
Adam34		atgagtgggactaaggccctg	gcggttatgatctattactac	

*Position of 5′-most nucleotide of region 1 was arbitrarily designated as '1'.

RESULTS

Association of mammalian PcG proteins to the *Hoxb8* genomic region at 12.5 dpc

First, the issue of whether PcG-silencing of Hox genes in developing embryos involves the direct binding of PcG gene products to Hox genes was addressed. PcG associations at genomic regions flanking *Hoxb8* were compared between transcriptionally repressed cranial and active caudal tissues by ChIP using embryonic tissues at 12.5 dpc. As the rostral boundary of *Hoxb8* expression is at the level of the 7th prevertebrae in the paraxial mesoderm and at the caudal hindbrain in the neural tube, embryos were dissected transversely at the levels of the pinna primordium and posterior edges of the forelimb buds, after the removal of internal viscera and hindlimb buds. Only cranial and caudal tissues were subjected to the analysis (Fig. 1A). Chromatin fractions of the respective embryonic tissues were purified and subjected to immunoprecipitation using antibodies against Rnf2, Phc1, Ring1, Cbx2 and Rnf110 (see Fig. S1 in the supplementary material) (Suzuki et al., 2002). Quantity of immunoprecipitated genomic DNA was measured by referring to serially diluted genomic DNA isolated from the initial lysates (see Fig. S2A in the supplementary material). Usually, for a given volume of chromatin fraction, the amount of DNA immunoprecipitated by anti-Rnf2 antibodies was four- to eightfold higher than that brought down in the absence of primary antibody (see Fig. S2A in the supplementary material). Amounts of DNA from respective tissues were further adjusted by PCR for the *tbx2* gene, which is also bound by Rnf2 in embryonic tissues (see Fig. S2B in the supplementary material). Equivalent amounts of DNA immunoprecipitated from the anterior and posterior tissues were subjected to semi-quantitative PCR using pairs of primers defining discrete regions in the *Hoxb* locus (Fig. 1F, top; see Table 2). Serially diluted genomic DNA isolated from the initial lysates was also subjected to the PCR to evaluate the enrichment value for each region of *Hoxb8* in immunoprecipitated materials (Fig. 1B-E). The *adam34* gene, which is expressed exclusively in adult testes, is not bound by any of Rnf2, Ring1, Phc1, Cbx2 or Rnf110 in embryonic tissues and thus turned out to serve as a negative control (Brachvogel et al., 2002) (Fig. 1B-E).

The association of Rnf2 with regions 1, 2, 3, 9, 10, 11, 13, 15, 16 and D1 was more than four times different in cranial and caudal tissues, whereas this was not the case for regions 4, 5, 6, 7, 8, 12, 14, 19, 20, 21, 22, 23, 24, 25 or D2 (Fig. 1B,F, Supplemental Fig. 3). In region 17 and 18, no significant association of Rnf2 was observed. Regions 1 and 2, and 10 and 11, correspond to the *Hoxb8* regulatory regions BH1100 and KA that have previously been identified by transgenic approaches; regions 3 and 13 include the promoters of *Hoxb8* and *Hoxb7*, respectively (Charité et al., 1995; Vogels et al., 1993). Therefore, Rnf2 differentially binds to the proximal cis-regulatory elements of 5′ *Hoxb* genes in cranial and caudal embryonic tissues. Likewise, a significant differential association of Rnf2 to the distal element (DE) located between *Hoxb4* and *Hoxb5*

(Oosterveen et al., 2003) was also seen in cranial and caudal tissues. Similar to Rnf2, Ring1 association was seen in cranial tissues, except for regions 3 and 7 (Fig. 1D). In contrast to Rnf2 binding, the association of Phc1 extended through all regions examined except for region 8, without any obvious differences between cranial and caudal tissues (Fig. 1C). Nevertheless, in region 3, the association did appear to be significantly stronger in the caudal tissues. Furthermore, there was no significant difference between cranial and caudal tissues with respect to the chromatin association of Cbx2 (Fig. 1D). Therefore, these results indicate that Phc1 and Cbx2 are bound to *Hoxb8* genomic region irrespective of the transcriptional state of the gene. Rnf110 association to regions 3 and 10 was seen in the cranial tissues only, but to regions 1, 2, 7 and 14 it was seen in both cranial and caudal tissues (Fig. 1E). These experiments were

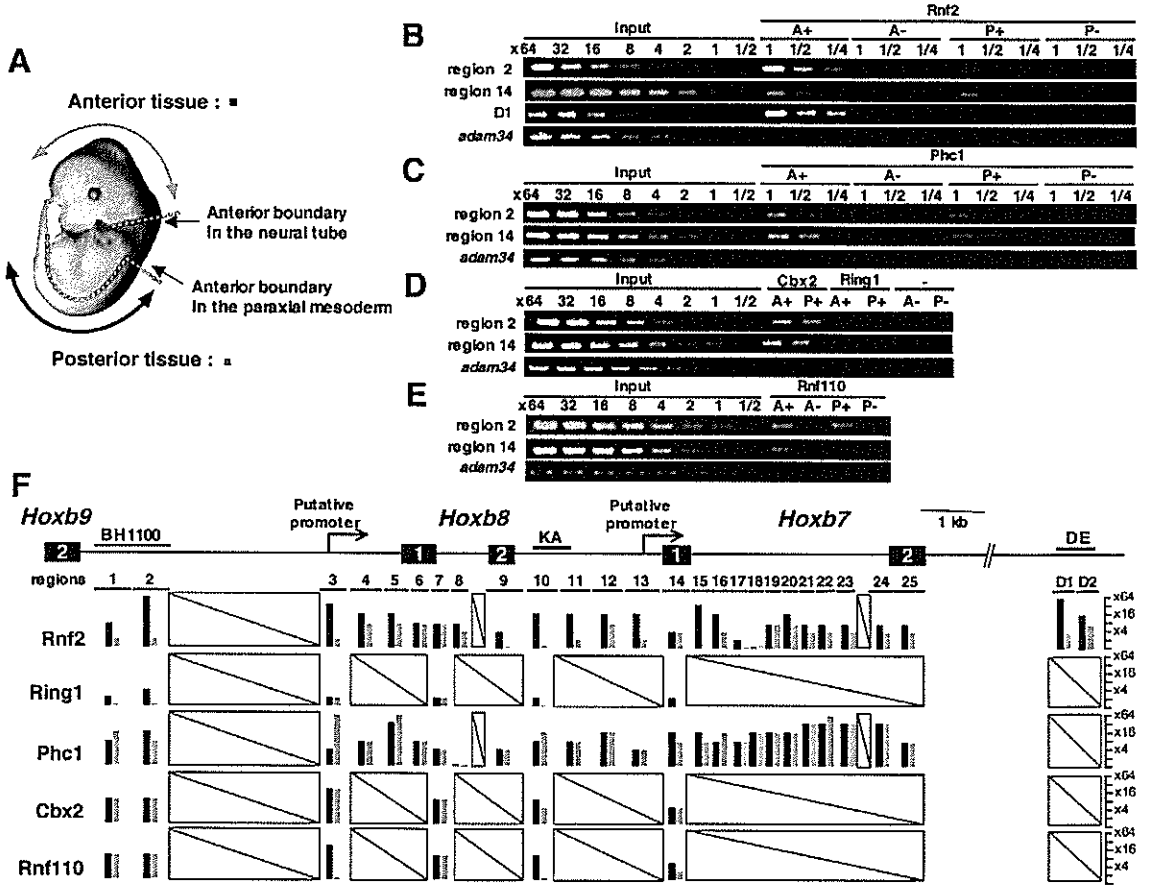

Fig. 1. Comparison of PcG associations with *Hoxb8* genomic surrounding at 12.5 dpc between anterior and posterior tissues. (**A**) Embryonic tissues used in this study. Wild-type embryos at 12.5 dpc were dissected as illustrated and anterior (A) and posterior (P) tissues (paraxial mesoderm plus neuroectoderm) were subjected to the ChIP analyses. (**B**) Comparative analysis of Rnf2 association to regions 2, 14 and D1 between anterior and posterior tissues. The chromatin fraction purified from A or P tissue was subjected to the immunoprecipitation with anti-Rnf2 antibody. Amounts of genomic DNA immunoprecipitated by anti-Rnf2 (A+ or P+) were quantified by comparing with serially diluted genomic DNA isolated from the original chromatin fractions designated as 'Input' (see Fig. S2A in the supplementary material) and equivalent amounts of immunoprecipitated DNA to that of 'Input' DNA loaded into lane 1 were subjected to PCR reactions. Usually 10 to 20 ng of genomic DNA was used. Immunoprecipitated DNA was also serially diluted. Mock-immunoprecipitated DNA (A– and P–) derived from the same volume of the chromatin fraction as used for anti-Rnf2 immunoprecipitation were subjected to the PCR. The *adam34* locus was used as a negative control. (**C**) Comparative analysis of Phc1 association to regions 2 and 14 between anterior and posterior tissues. (**D**) Comparative analyses for association of Cbx2 and Ring1 to regions 2 and 14. Amounts of genomic DNA (A+ and P+) immunoprecipitated by anti-Cbx2 and anti-Ring1 antibodies subjected to PCR were equivalent to that of 'Input' DNA loaded into lane 1. Mock-immunoprecipitated DNA (A– and P–) derived from the same volume of the chromatin fraction as used for anti-Cbx2 and -Ring1 immunoprecipitation were subjected to the PCR. (**E**) Rnf110 association to regions 2 and 14. All experiments were conducted as described using anti-Rnf110 antibody. (**F**) Schematic comparisons of Rnf2, Ring1, Phc1, Cbx2 and Rnf110 association to the *Hoxb8* genomic surrounding between anterior and posterior tissues. Genomic organization around *Hoxb8* gene is shown at the top. Exonic regions are indicated by black boxes and the exon numbers are numerically shown in the boxes. Positions of known cis-acting regulatory elements are represented by overlying bold bars indicated as BH1100, KA and DE (Charité et al., 1995; Vogels et al., 1993; Oosterveen et al., 2003). Putative promotor regions are indicated by folded arrows. The genomic regions examined by PCR using specific primer pairs listed in Table 1 are shown by bars and numerically indicated. The relative quantity of each genomic region in immunoprecipitated genomic DNA from anterior and posterior tissues was estimated by referring to 'Input' DNA isolated from the initial lysates and enrichment values against the 'Input', and are represented by the black and gray bars, respectively. Genomic regions left unexamined are covered by boxes crossed with a diagonal line.

performed three times with similar results (see Fig. S3 in the supplementary material). In summary, the complete form of the class 2 PcG complexes predominantly associate with *Hoxb8* in tissues where the gene is repressed, whereas form(s) lacking at least the Rnf2 component also bind in tissues actively expressing the Hox gene.

Differences between H3-K9 acetylation and H3-K27 trimethylation at *Hoxb8* in cranial and caudal embryonic tissues

Following this, the issue of the degree of H3-K9 acetylation and H3-K4 methylation at *Hoxb8* genomic regions in expressing and non-expressing embryonic tissues, was addressed. These epigenetic marks have been shown to be one of the prerequisites for the efficient recruitment of TBP through the interaction of TAF1 with the H3-K9 and K14 acetylated residues (Agalioti et al., 2002). A linear correlation between histone modifications and the transcriptional state of Hox genes has been seen in developing embryos at *Hoxd4* locus and MEFs that are derived from *Mll* mutants and wild-type controls (Rastegar et al., 2004; Milne et al., 2002). Therefore, as H3-K9 acetylation and H3-K4 methylation may be prerequisites for active transcription of Hox genes, these extents were compared between anterior and posterior embryonic tissues. H3-K9 acetylation and H3-K4 methylation around the *Hoxb8* was more abundant in the transcriptionally active caudal embryonic part than in the non-expressing anterior part as reported by Rastegar et al. (Rastegar et al., 2004) (Fig. 2A,B).

The methylation of H3-K9 and H3-K27 constitutes imprints for transcriptionally silent chromatin and is involved in many functions, including the formation of centromeric heterochromatin, X inactivation, PcG-mediated gene silencing and transcriptional repression at euchromatic positions (Fischle et al., 2003; Lachner et al., 2003). In particular, trimethylation of H3-K27 has been shown to be mediated by class 1 PcG complexes (Cao et al., 2002). The degree of H3-K9 and H3-K27 methylation at regions 2, 3 and 8 was compared between cranial and caudal embryonic regions. At all the regions examined, H3-K27 trimethylation was more abundant in the transcriptionally silent cranial embryonic part than in the Hox-expressing caudal part (Fig. 2B). No significant levels of di- or trimethylation of H3-K9 or dimethylation of H3-K27 were seen at any of the regions examined (Y.F. and H.K., unpublished).

Developmental kinetics of Rnf2-association and of histone H3 modifications at *Hoxb8*

Loss of spatial restriction of *Hoxb6* expression, between 8.5 and 9.5 dpc, has been reported as resulting from the *Rnf110/Bmi1* double mutation (Akasaka et al., 2001). Similarly, *Mll* deficiency progressively silences Hox gene expression within this time window

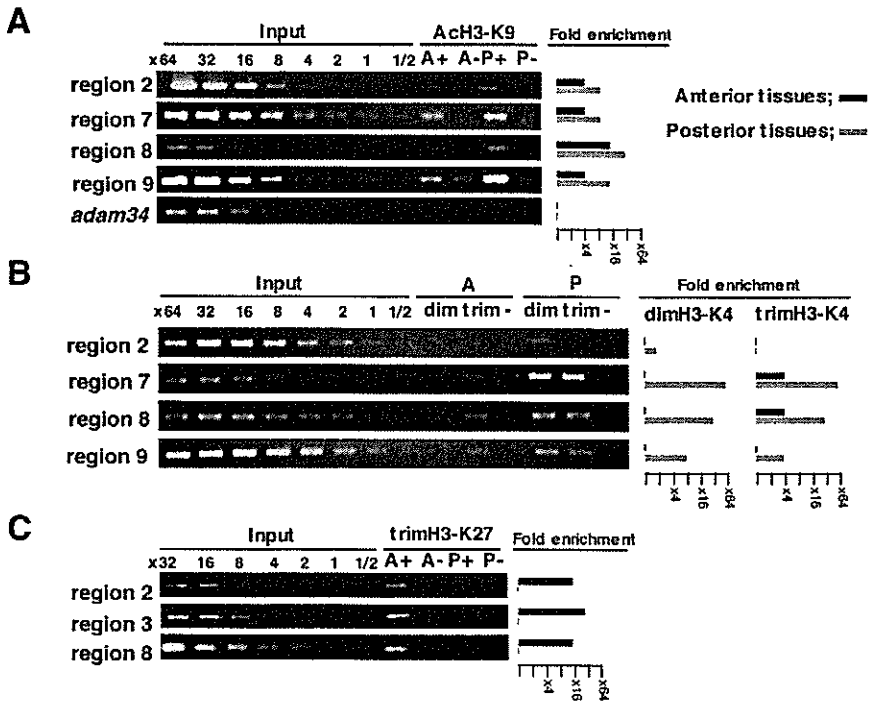

Fig. 2. Comparison of H3-K9 acetylation, H3-K4 methylation and H3-K27 trimethylation in *Hoxb8* genomic surrounding at 12.5 dpc between anterior and posterior tissues. (**A**) Comparative analysis of H3-K9 acetylation at regions 2, 7, 8 and 9. (Left) Whole-cell lysates (WCE) prepared from anterior and posterior parts of 12.5 dpc embryos were subjected to ChIP analyses by using anti-acetylated H3-K9. Amounts of immunoprecipitated genomic DNA (A+ and P+) by anti-acetylated H3-K9 subjected to PCR were equivalent to that of 'Input' DNA loaded in lane 1. Mock-immunoprecipitated DNA (A– and P–) derived from the same volume of the chromatin fraction as used for anti-acetylated H3-K9 immunoprecipitation were subjected to the PCR. (Right) Schematic comparison of H3-K9 acetylation between anterior and posterior tissues. The relative quantity of each genomic region in immunoprecipitated genomic DNA from anterior and posterior tissues was estimated by referring to 'Input' DNA isolated from the initial lysates and enrichment values against the initial lysate are represented by the black and gray bars, respectively. (**B**) Comparative analysis of di- and trimethylation of H3-K4 at the region 2, 7, 8 and 9. Representative results (left) and schematic summary (right) are shown. (**C**) Comparative analysis of trimethylation of H3-K27 at the region 2, 3 and 8. Representative results (left) and schematic summary (right) are shown.

(Yu et al., 1998). This suggests that this developmental stage might be the crucial period when PcG association and H3-K9 acetylation at *Hoxb8* play their role in modulating gene expression.

Prior to the ChIP analyses, we re-examined the expression of *Hoxb8* gene in the cranial and caudal tissues in quantitative manner by using real-time PCR (Fig. 3A). As reported previously by extensive in situ hybridization analyses, caudally restricted expression of *Hoxb8* was already established at 8.0 dpc and its relative quantity progressively increased until 12.5 dpc (Deschamps and Wijgerde, 1993). We carried out the kinetic analyses of the Rnf2 association, H3-K9 acetylation and H3-K27 trimethylation in early to later developmental stages across the *Hoxb8* promoter region (region 3 in Fig. 1F). In 8.0 dpc embryos, no Rnf2 association was seen at the six-somite stage. It was first seen, exclusively in cranial tissue, at the eight-somite stage (Fig. 3B). This was also the case at later stages up to 12.5 dpc (Fig. 3C-E). The relative quantity of Rnf2 association gradually increased and reached a maximal level at 10.5 dpc (Fig. 3E). H3-K9 acetylation was observed in the cranial region at the six-somite stage and in both cranial and caudal regions at the eight-somite stage. It was present at higher levels in the caudal region in 9.5 and 10.5 dpc embryos than in 8.0 dpc. H3-K27 trimethylation at region 3 continued to be seen in the cranial, but not in the caudal, region from 8.5 to 12.5 dpc. In summary, a differential association of Rnf2 with the *Hoxb8* promoter region, region 3, was established from 8.0 dpc onwards, and reached completion around 10.5 dpc (Fig. 3G) (Deschamps and Wijgerde, 1993). Relative amounts of acetylated H3-K9 in this region also increased up to 12.5 dpc. Likewise, differential trimethylation of H3-K27 was already established at 9.5 dpc and maintained to 12.5 dpc. These observations indicate that the Rnf2 association, H3-K9 acetylation and H3-K27 trimethylation may be involved to maintain the spatially restricted expression of the *Hoxb8*.

Evidence for the role of Rnf2 in transcriptional repression of Hox genes

Differential association of Rnf2 to *Hoxb8* genomic surrounding in tissues not expressing *Hoxb8* suggests its repressive role in *Hoxb8* transcription. This hypothesis is supported by our previous

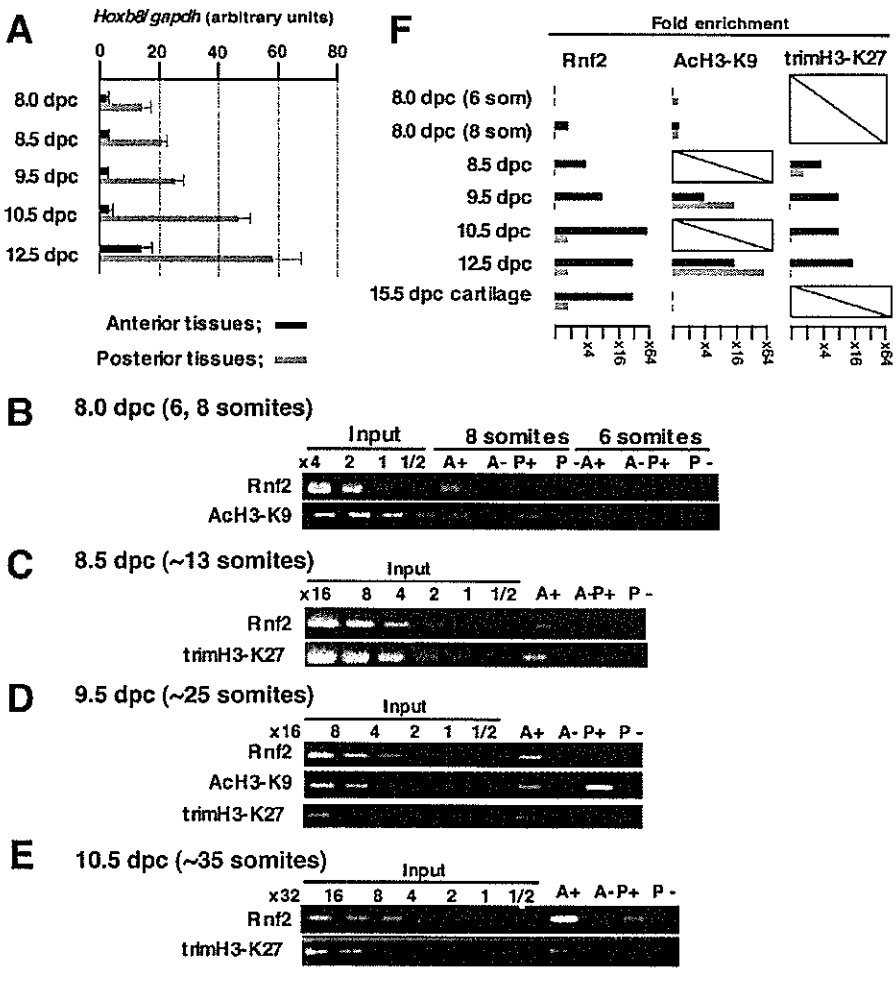

Fig. 3. Temporal changes in Rnf2 association, H3-K9 acetylation and H3-K27 trimethylation at the *Hoxb8* putative promotor region. (**A**) The expression of *Hoxb8* in the cranial and caudal tissues at various developmental stages, as quantified by using real-time PCR against the expression of *Gapdh*. Relative quantity was compared between anterior and posterior tissues. The *Hoxb8/Gapdh* ratio in the anterior tissue of 8.0 dpc embryo was arbitrarily 1. Embryos were bisected into the anterior and posterior tissues as described below. (**B**) Six- and eight-somite embryos were bisected at the level of the newly generated somite boundary and separated into anterior segmented (A) and posterior unsegmented (P) regions, and WCE prepared from respective tissues were subjected to ChIP analyses. (**C**) Embryos at the ~13-somite stage were dissected into three pieces at the boundary between somites 9 and 10, and at the newly generated somite boundary. WCE prepared from cranial region up to somite 9 (A) and posterior unsegmented region (P) were subjected to ChIP analyses. (**D**) Embryos at 9.5 dpc (about 25 somites) were bisected into anterior (A) and posterior (P) pieces at the level of somite 9/10 boundary and respective WCE were subjected to ChIP analyses. (**E**) Embryos at 10.5 dpc (~35 somites) were dissected at the level of the posterior end of the hindbrain and caudally to the forelimb bud after removing the viscera. For ChIP using anti-Rnf2, chromatin fractions prepared from the anterior (A) and posterior (P) tissues were used, whereas WCE were used for anti-acetylated H3-K9 and -trimethylated H3-K27 antibodies. (**F**) Schematic comparisons of Rnf2 association, H3-K9 acetylation and H3-K27 trimethylation at the region 3 between anterior and posterior tissues. The relative quantity of each genomic region in immunoprecipitated genomic DNA from anterior and posterior tissues was estimated by referring to those of 'Input' DNA isolated from the initial lysates and enrichment values against the 'Input' are represented by the black and gray bars, respectively. Stages left unexamined are indicated by boxes crossed with a diagonal line.

experiments that used an hypomorphic allele of *Rnf2*, in which the de-repression of several Hox genes was seen at 11.5 dpc (Suzuki et al., 2002). However, it was not determined whether Rnf2 association was functionally involved in the maintenance rather than early establishment of this repressed status. To address this question, we conditionally depleted functional *Rnf2* after the expression domain of *Hoxb8* was established. Because of early embryonic lethality of *Rnf2*-null mice, we generated a conditional allele designated as $Rnf2^{fl}$ in which exon 2, containing the ATG initiation codon, was flanked with loxP sites (Voncken et al., 2003; de Napoles et al., 2004). Primary MEFs were derived from the cranial part of $Rnf2^{fl/fl}$ 9.5 dpc embryos in which *Hoxb8* expression was repressed. Subsequent deletion of *Rnf2* was achieved by infection of MEF cultures with adenovirus expressing the CRE recombinase (Ad-Cre) as described (de Napoles et al., 2004). Rnf2 depletion was evident in western analysis of infected cell culture (Fig. 4A) and took 2 days for completion. The analysis of *Hoxb8* expression continued for 4 days after Ad-Cre infection. Two independent experiments demonstrated more than a 16-fold increase of *Hoxb8* expression in infected MEFs compared with the uninfected control. Therefore Rnf2 association is essential for the maintenance of the transcriptional repression of *Hoxb8*.

After this, the repressive role of Rnf2 in undifferentiated embryonic stem (ES) cells was investigated because Hox repression was accompanied by both chromatin condensation of the Hox cluster and the location of the Hox genes within the chromosome territory, whereas decondensation and reorganization accompanied Hox gene expression both in ES cells and the developing neural tube (Chambeyron and Bickmore, 2004; Chambeyron et al., 2005).

Seven $Rnf2^{fl/fl}$ ES cells have been derived (de Napoles et al., 2004). $Rnf2^{-/-}$ ES cell derivatives of one of these lines, the male ES cell line, 13-3, were generated by CRE-mediated excision of exon 2 (Fig. 4B). Loss of functional Rnf2 resulted in de-repression of *Hoxa1*, *Hoxa7*, *Hoxb3*, *Hoxb8*, *Hoxb13*, *Hoxc9*, *Hoxd8* and *Hoxd10* but not of *Hoxc8* (Fig. 4C). To test if de-repression of Hox genes is a direct consequence of mutating Rnf2, complementation experiments were carried out, transfecting mutant ES cells with a construct expressing Myc-tagged Rnf2. As shown in Fig. 4B, transfected mutant ES cells expressed transgene-encoded Rnf2 at a level equivalent to half that of endogenous Rnf2. RT-PCR analysis revealed that the expression of *Hoxa1*, *Hoxb3*, *Hoxb8* and *Hoxd8* was repressed albeit not to the same degree as in the parental $Rnf2^{fl/fl}$ ES cells (Fig. 4C). These results confirm that Rnf2 association is required to mediate the transcriptional repression of Hox genes in ES cells.

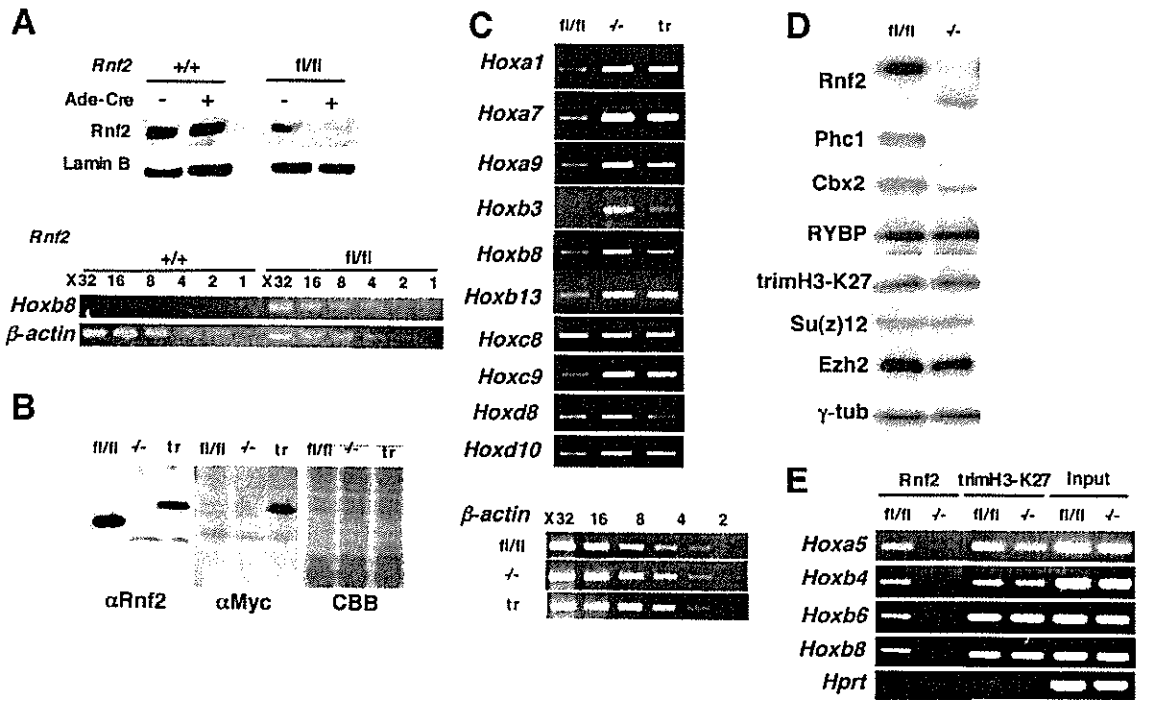

Fig. 4. De-repression of Hox genes in $Rnf2^{-/-}$ MEFs and ES cells. (**A**) Conditional depletion of Rnf2 lead to de-repression of *Hoxb8* in MEFs derived from the cranial part of $Rnf2^{fl/fl}$ 9.5 dpc embryos. (Top) Infection of Cre-expressing adenovirus vector to MEFs derived from $Rnf2^{fl/fl}$ embryos (fl/fl) depleted the Rnf2 gene products, whereas the wild-type (+/+) MEFs were unaffected. Lamin B was used as a control. (Bottom) The expression of Hoxb8 was induced by infection of Cre-expressing adenovirus vector in $Rnf2^{fl/fl}$ MEFs (fl/fl), but not in the wild type (+/+). (**B**) $Rnf2^{-/-}$ (–/–) ES cells were derived from $Rnf2^{fl/fl}$ (fl/fl) ES cells by transient overexpression of Cre-recombinase. Rnf2 was re-expressed by transfecting $Rnf2^{-/-}$ ES cells with a construct expressing Myc-tagged Rnf2 (tr). The expression of endogenous and transfected Rnf2 was examined by using anti-Rnf2 (left) and -Myc (middle) antibodies. CBB staining was used as a loading control (right). (**C**) The expression of Hox cluster genes in $Rnf2^{fl/fl}$ (fl/fl), $Rnf2^{-/-}$ (–/–) and Rnf2 transfected (tr) ES cells was compared by RT-PCR. The quantity of synthesized cDNA from respective cells was equalized by comparing the relative amounts of β-actin transcripts. (**D**) The expression of Phc1 and Cbx2 gene products was reduced in $Rnf2^{-/-}$ ES cells (–/–) in comparison with the wild type (fl/fl), whereas the expression of RYBP (another Rnf2-binding protein that is not found in hPRC-H complex or class 1 PcG proteins) was not altered. (**E**) Rnf2 association and H3-K27 trimethylation at Hox promoter regions were compared between $Rnf2^{fl/fl}$ and $Rnf2^{-/-}$ ES cells. For the 'Input', genomic DNA extracted from the original whole cell lysate equivalent to the 1/40 volume of that used for the ChIP analysis was subjected to the PCR. *Hprt* was used as a negative control.

Next, the method by which Rnf2 deficiency impacts on the functions of class 2 PcG complexes was investigated. As it has been suggested that Ring1 is an important component in the stabilization of the Polycomb core complex in Sf9 cells (Francis et al., 2001), the expression levels of other components of class 2 PcG complexes in *Rnf2*$^{-/-}$ ES cells was examined. The expression of both Phc1 and Cbx2 gene products was obviously reduced in *Rnf2*$^{-/-}$ ES cells (Fig. 4D; M.E. and H.K., unpublished). By contrast, the expression of RYBP, another Rnf2-binding protein, which is not found in hPRC-H complex, was not altered (Garcia et al., 1999) (Fig. 4D). As the transcription of *Phc1* and *Cbx2* was not altered in *Rnf2*$^{-/-}$ ES cells, Rnf2 loss specifically affects the expression of Phc1 and Cbx2. It is thus likely that Rnf2 impacts the Hox expression by regulating the stability of the class 2 PcG complexes.

The coincidence of Rnf2 association and H3-K27 trimethylation in transcriptionally repressed region further prompted us to ask whether de-repression of Hox genes in *Rnf2*$^{-/-}$ ES cells involves a change of H3-K27 trimethylation across the Hox genomic regions. The expression of Suz12 and Ezh2 were not significantly changed in *Rnf2*$^{-/-}$ ES cells (Fig. 4D). Concordant with this result, ChIP analyses revealed that local level of H3-K27 trimethylation at Hox promoter regions were almost unchanged (Fig. 4E). Therefore, Rnf2 deficiency affects Hox gene expressions without changing local H3-K27 trimethylation.

Functional involvement of trimethylated H3-K27 on Rnf2 association at Hox loci and on Hox gene expression

In *Drosophila*, trimethylation on H3-K27 has been shown to facilitate the recruitment of class 2 PcG complexes via direct interaction between trimethylated H3-K27 and the chromodomain of Pc (Cao et al., 2002; Czermin et al., 2002; Muller et al., 2002). Therefore, Hox gene expression and Rnf2 association at the *Hoxb* locus, in the absence of trimethylated H3-K27, was examined using *Suz12*$^{-/-}$ ES cells. We have independently generated a loss-of-function allele of *Suz12* and the homozygous mutants exhibited a phenotype almost identical to that reported by Pasini et al. (Pasini et al., 2004) (K.I. and H.K., unpublished). *Suz12*$^{-/-}$ ES cells were derived from crosses of heterozygous mutants. The absence of Suz12 reduced the levels of H3-K27 tri- and dimethylation to less than 10% of the wild type but did not significantly change H3-K9 methylation (Pasini et al., 2004). First, the association of class 1 PcG and H3-K27 trimethylation at the Hox promotor regions was investigated. Anti-Suz12, -Eed and -trimethylated H3-K27 antibodies specifically immunoprecipitated significant amounts of Hox promoter fragments from the wild-type ES cells (Fig. 5A). In *Suz12*$^{-/-}$ ES cells, no Hox DNA could be detected at all upon anti-Suz12 immunoprecipitation. The loss of Suz12 significantly reduced Eed association and H3-K27 trimethylation at Hox genes. Therefore, class 1 PcG complexes associate locally to Hox genes and mediate local H3-K27 trimethylation in undifferentiated ES cells. Second, the expression of *Hoxa1*, *Hoxa4*, *Hoxb1*, *Hoxb3*, *Hoxb4*, *Hoxb6*, *Hoxb8*, *Hoxb9* and *Hoxc6* was compared between wild-type and *Suz12*$^{-/-}$ ES cells by RT-PCR. *Suz12*$^{-/-}$ ES cells were shown to express more Hox gene transcripts than the wild type (Fig. 5B). Therefore, local H3-K27 trimethylation mediated by class 1 PcG complexes, or association of the complexes, are likely to be required in order to mediate repression of Hox genes. We went on to examine Rnf2 association in *Suz12*$^{-/-}$ ES cells. Rnf2 association to the Hox promoters was significantly reduced in *Suz12*$^{-/-}$ ES cells (Fig. 5A). Therefore H3-K27 trimethylation may be a prerequisite for the association of Rnf2 with Hox regulatory regions, as already demonstrated in *Drosophila*. The role of class 1 PcG complexes in the recruitment of the class 2 complexes via protein-protein interactions is not necessarily excluded.

The positive role of PcG complexes on transcription is coupled to increased H3-K9 acetylation

Results from this study also show that PcG gene products associate to *Hoxb8* genomic regions in the transcriptionally active caudal embryonic tissues. This is in line with the recently uncovered positive function of class 2 PcG complexes (de Graaff et al., 2003). Null mutations in the *Rnf110* and *Phc1* loci have been shown to decrease the transcription level of endogenous *Hoxb1*, and to severely impair the transcription from Hox/*lacZ* reporters and knock-in loci (de Graaff et al., 2003). In addition, a positive action of PcG complexes explains the drop in gene expression levels within the *Hoxb8* expression domains known to occur around 9.5 dpc in *Bmi1/Rnf110* and *Phc1/Phc2* double mutants (Akasaka et al., 2001; de Graaff et al., 2003; Isono et al., 2005b). As the level of histone H3 acetylation correlates with Hox gene expression in *Mll* mutants and controls, and Mll and Bmi1 proteins display discrete subnuclear colocalization, we investigated whether the drop in *Hoxb8* expression level in *Rnf110/Bmi1* and *Phc1/Phc2* double mutants involved a change in H3-K9 acetylation (Hanson et al., 1999; Milne et al., 2002; de Graaff et al., 2003). The degree of H3-K9 acetylation in the caudal region of *Rnf110*$^{-/-}$*Bmi1*$^{-/-}$ embryos was much lower

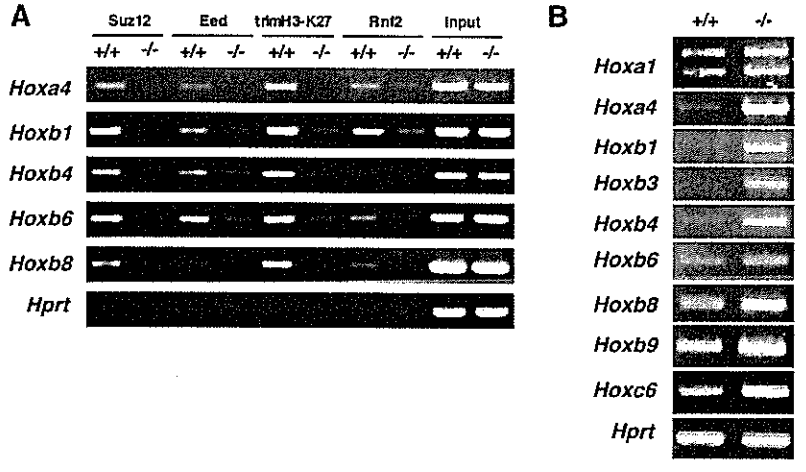

Fig. 5. De-repression of Hox genes in *Suz12*$^{-/-}$ ES cells correlates with reduction of Rnf2 association to Hox genomic regions. (**A**) The association of Suz12, Eed, Rnf2 and H3-K27 trimethylation at the Hox promoter regions in the wild-type and *suz12*$^{-/-}$ ES cells. Whole-cell lysates prepared from approximately the same number of wild type (+/+) and *suz12*$^{-/-}$ (–/–) ES cells were subjected to ChIP analyses using anti-Suz12, -Eed, -trimethylated H3-K27 and -Rnf2 antibodies. For the 'Input', genomic DNA extracted from the original whole cell lysate equivalent to the 1/40 volume of that used for the ChIP analysis was subjected to the PCR. *Hprt* was used as a control. (**B**) The expression of Hox cluster genes in the wild type (+/+) and *suz12*$^{-/-}$ (–/–) ES cells was compared by RT-PCR.

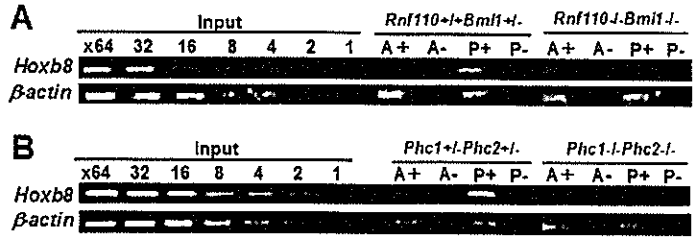

Fig. 6. Decreased H3-K9 acetylation at the first exonic region of *Hoxb8* in the posterior tissues of *Rnf110*$^{-/-}$*Bmi1*$^{-/-}$ and *Phc1*$^{-/-}$*Phc2*$^{-/-}$ embryos at 9.5 dpc. (A) Degree of H3-K9 acetylation in the anterior (A) and posterior (P) regions were compared in *Rnf110*$^{+/-}$*Bmi1*$^{+/-}$ and *Rnf110*$^{-/-}$*Bmi1*$^{-/-}$ embryos. The β-actin promoter was used as a positive control. (B) Degree of H3-K9 acetylation in the anterior (A) and posterior (P) regions were compared in *Phc1*$^{-/-}$*Phc2*$^{+/-}$, *Phc1*$^{+/-}$*Phc2*$^{-/-}$ and *Phc1*$^{-/-}$*Phc2*$^{-/-}$ embryos. The β-actin promoter was used as a positive control. In this study, the negative control ChIPs (A– and P–) were performed with rabbit IgG.

than in *Rnf110*$^{+/+}$*Bmi1*$^{+/-}$, whereas the H3-K9 acetylation at the β-actin promoter was almost equivalent (Fig. 6A). Similarly, H3-K9 acetylation level in the caudal part of *Phc1*$^{-/-}$*Phc2*$^{-/-}$ was equivalent to the cranial part whereas craniocaudally graded acetylation was seen in *Phc1*$^{+/-}$*Phc2*$^{+/-}$ embryos (Fig. 6B). Therefore association of class 2 PcG gene products to *Hox*b8 is required for the maintenance of H3-K9 acetylation in transcriptionally active regions.

DISCUSSION

The main outcome of this study was to show that binding of a specific, Rnf2-containing form of the class 2 PcG complex, as well as H3-K27 trimethylation marking inactive chromatin, correlates with the maintenance of transcriptional silencing of a Hox gene in developing embryos. Moreover, the results demonstrated that genetic impairment of both PcG binding, and H3-K27 trimethylation leads to Hox gene derepression, and that H3-K27 trimethylation is required for PcG binding. In addition, we showed that the establishment of differential PcG binding and histone marks in expressing and non-expressing embryonic tissues occur in the same developmental time window as when Hox genes are deregulated in *PcG* mutants.

Rnf2 association to known regulatory elements of the *Hoxb8* gene is seen predominantly in transcriptionally silent anterior embryonic tissues, whereas the binding of other PcG class 2 members, Phc1 and Cbx2, is observed at all AP levels, irrespective of transcriptional status. This implies that different forms of class 2 PcG complexes bind to the Hoxb genomic region in embryonic domains where the gene is transcriptionally active and repressed. This is reminiscent of previous findings in the *Engrailed/Inv/GeneVI* complex in *Drosophila* SL-2 cells, where the Pc protein is exclusively associated with transcriptionally silent genes, while Ph and Psc are present irrespective of the transcriptional status (Strutt and Paro, 1997). Therefore the complete, 'perfect' form of the class 2 PcG core complex may mediate transcriptional repression more efficiently than form(s) lacking the Rnf2 component. If this is the case, incorporation of the Rnf2 component into the complex might be a limiting process to mediate transcriptional repression and regulate its stability (Francis et al., 2001). It is also possible that the role of Rnf2 is mediated through its E3 ubiquitin ligase activity directed to histone H2A (Wang et al., 2004a; de Napoles et al., 2004).

Transcriptional repression of Hox genes in the developing embryo has been shown to correlate with the association of Rnf2-containing class 2 PcG complexes and H3-K27 trimethylation. De-repression of Hox genes in *Rnf2* and *Suz12* mutant cells reveal the requirement of both Rnf2 association and H3-K27 trimethylation in the mediation of this transcriptional repression. As Rnf2 association to Hox genes is reduced in *Suz12* mutant ES cells and *Rnf2* mutation alters Hox expression without changing local levels of H3-K27 trimethylation, H3-K27 trimethylation mediated by class 1 PcG complexes at Hox genes may facilitate subsequent binding of Rnf2-containing PcG complexes. Recruitment of Rnf2-containing PcG complexes may in turn prevent the access of nucleosome remodeling factors, such as SWI/SNF complex, leading to the formation of a repressed chromatin status (Shao et al., 1999; Levine et al., 2002). Therefore, molecular circuitry underlying PcG silencing of Hox genes seems to have been evolutionarily conserved between *Drosophila* and mammals. It is also notable that Cbx2, a homologue of *Drosophila* Pc, binds to *Hoxb8* in transcriptionally active embryonic tissues, despite the lack of histone H3 trimethylated at K27. This is consistent with previous biochemical data that have shown the association of purified or reconstituted PcG complexes with the nucleosomal templates lacking histone tails (Shao et al., 1999). The implication of these findings is that there are at least two different means by which class 2 PcG complexes bind to the chromatin, and that the association, which involves trimethylated H3-K27, mediates the repression at the Hox genes in vivo (Cao et al., 2002; Czermin et al., 2002; Muller et al., 2002).

The maintenance of regionally restricted expression of Hox genes is likely to involve H3-K9 acetylation and H3-K4 methylation (Milne et al., 2002; Rastegar et al., 2004). We have shown that these modifications of the histone tail increases craniocaudally along the axis. Although the transcriptionally active posterior tissues of 9.5 dpc and older embryos are more heavily acetylated at H3-K9 than the anterior, non-Hox expressing tissues, some acetylation of H3-K9 at *Hoxb8* is seen in anterior regions where *Hoxb8* expression is repressed at early and later developmental stages. De-repression of *Hoxb8* expression upon depletion of Rnf2 in MEFs derived from the cranial part of 9.5 dpc embryos suggests the involvement of Rnf2-containing class 2 PcG complexes to mediate this transcriptional repression. Therefore, our data suggest that the associations of Rnf2-containing PcG complexes and acetylated H3-K9 may counteract each other and cooperate to maintain the anterior boundaries of *Hoxb8* expression at mid-gestational stages and later. This is consistent with the antagonistic properties of *Mll* and *Bmi1* mutations (Hanson et al., 1999). Moreover, the establishment of the differential binding of the Rnf2 and H3-K9 acetylation at *Hoxb8* during embryogenesis temporally coincides with de-repression of that Hox gene in *Bmi1/Rnf110* and *Phc1/Phc2* double homozygotes, and loss of its transcription in *Mll* homozygotes (Akasaka et al., 2001; Yu et al., 1998; Isono et al., 2005b). Intriguingly, class 2 PcG complexes, which lack the Rnf2 component, are also involved in the maintenance of H3-K9 acetylation in embryonic tissues where Hox genes are expressed. This is consistent with predominant subnuclear localization of several PcG proteins in the perichromatin compartment where most pre-mRNA synthesis takes place (Cmarco et al., 2003). The molecular mechanisms underlying this positive action remain unaddressed.

In conclusion, class 2 PcG gene products play distinct roles in embryonic territories, which are silent or active for *Hoxb8* transcription, by forming complexes of different composition. Interaction between class 1 and class 2 PcG complexes mediated by

trimethylated H3-K27 play decisive roles in Hox gene repression outside their expression domains, as seen in *Drosophila*. In addition, within the Hox expression domain, class 2 PcG complexes are involved in maintaining a transcriptionally active status, independent of H3-K27 trimethylation.

Supplementary material

Supplementary material for this article is available at http://dev.biologists.org/cgi/content/full/133/12/2371/DC1

References

Agalioti, T., Chen, G. and Thanos, D. (2002). Deciphering the transcriptional histone acetylation code for a human gene. *Cell* **111**, 381-392.

Akasaka, T., Kanno, M., Mieza, M. A., Balling, R., Taniguchi, M. and Koseki, H. (1996). A role for mel-18, a Polycomb group-related vertebrate gene, during the anteroposterior specification of the axial skeleton. *Development* **122**, 1513-1522.

Akasaka, T., van Lohuizen, M., van der Lugt, N., Mizutani-Koseki, Y., Kanno, M., Taniguchi, M., Vidal, M., Alkema, M., Berns, A. and Koseki, H. (2001). Mice doubly deficient for the Polycomb Group genes Mel18 and Bmi1 reveal synergy and requirement for maintenance but not initiation of Hox gene expression. *Development* **128**, 1587-1597.

Atsuta, T., Fujimura, S., Moriya, H., Vidal, M., Akasaka, T. and Koseki, H. (2001). Production of monoclonal antibodies against mammalian Ring1B proteins. *Hybridoma* **20**, 43-46.

Brachvogel, B., Reichenberg, D., Beyer, S., Jehn, B., von der Mark, K. and Bielke, W. (2002). Molecular cloning and expression analysis of a novel member of the Disintegrin and Metalloprotease-Domain (ADAM) family. *Gene* **288**, 203-210.

Cao, R., Wang, L., Wang, H., Xia, L., Erdjument-Bromage, H., Tempst, P., Jones, R. S. and Zhang, Y. (2002). Role of histone H3 lysine 27 methylation in Polycomb-group silencing. *Science* **298**, 1039-1043.

Cavalli, G. and Paro, R. (1998). The Drosophila Fab-7 chromosomal element conveys epigenetic inheritance during mitosis and meiosis. *Cell* **93**, 505-518.

Chambeyron, S. and Bickmore, W. A. (2004). Chromatin decondensation and nuclear reorganization of the HoxB locus upon induction of transcription. *Genes Dev.* **18**, 1119-1130.

Chambeyron, S., Da Silva, N. R., Lawson, K. A. and Bickmore, W. A. (2005). Nuclear reorganization of the HoxB complex during mouse embryonic development. *Development* **132**, 2215-2223.

Charité, J., de Graaff, W., Vogels, R., Meijlink, F. and Deschamps, J. (1995). Regulation of the Hoxb-8 gene: synergism between multimerized cis-acting elements increases responsiveness to positional information. *Dev. Biol.* **171**, 294-305.

Cmarko, D., Verschure, P. J., Otte, A. P., van Driel, R. and Fakan, S. (2003). Polycomb group gene silencing proteins are concentrated in the perichromatin compartment of the mammalian nucleus. *J. Cell Sci.* **116**, 335-343.

Czermin, B., Melfi, R., McCabe, D., Seitz, V., Imhof, A. and Pirrotta, V. (2002). Drosophila enhancer of Zeste/ESC complexes have a histone H3 methyltransferase activity that marks chromosomal Polycomb sites. *Cell* **111**, 185-196.

de Graaff, W., Tomotsune, D., Oosterveen, T., Takihara, Y., Koseki, H. and Deschamps, J. (2003). Randomly inserted and targeted Hox/reporter fusions transcriptionally silenced in Polycomb mutants. *Proc. Natl. Acad. Sci. USA* **100**, 13362-13367.

de Napoles, M., Mermoud, J. E., Wakao, R., Tang, Y. A., Endoh, M., Appanah, R., Nesterova, T. B., Silva, J., Otte, A. P., Vidal, M. et al. (2004). Polycomb group proteins Ring1A/B link ubiquitylation of histone H2A to heritable gene silencing and X inactivation. *Dev. Cell* **7**, 663-676.

Deschamps, J. and Wijgerde, M. (1993). Two phases in the establishment of *Hox* expression domains. *Dev. Biol.* **152**, 473-480.

Fischle, W., Wang, Y. and Allis, C. D. (2003). Binary switches and modification cassettes in histone biology and beyond. *Nature* **425**, 475-479.

Francis, N. J., Saurin, A. J., Shao, Z. and Kingston, R. E. (2001). Reconstitution of a functional core polycomb repressive complex. *Mol. Cell* **8**, 545-556.

Garcia, E., Marcos-Gutierrez, C., del Mar Lorente, M., Moreno, J. C. and Vidal, M. (1999). RYBP, a new repressor protein that interacts with components of the mammalian Polycomb complex, and with the transcription factor YY1. *EMBO J.* **18**, 3404-3418.

Hamer, K. M., Sewalt, R. G., den Blaauwen, J. L., Hendrix, T., Satijn, D. P. and Otte, A. P. (2002). A panel of monoclonal antibodies against human polycomb group proteins. *Hybrid. Hybridomics* **21**, 245-252.

Hanson, R. D., Hess, J. L., Yu, B. D., Ernst, P., van Lohuizen, M., Berns, A., van der Lugt, N. M., Shashikant, C. S., Ruddle, F. H., Seto, M. et al. (1999). Mammalian Trithorax and polycomb-group homologues are antagonistic regulators of homeotic development. *Proc. Natl. Acad. Sci. USA* **96**, 14372-14377.

Isono, K., Mizutani-Koseki, Y., Komori, T., Schmidt-Zachmann, M. S. and Koseki, H. (2005a). Mammalian Polycomb-mediated repression of *Hox* genes requires the essential spliceosomal protein Sf3b1. *Genes Dev.* **19**, 536-541.

Isono, K., Fujimura, Y., Shinga, J., Yamaki, M., O-Wang, J., Takihara, Y., Murahashi, Y., Takada, Y., Mizutani-Koseki, Y. and Koseki, H. (2005b). Mammalian polyhomeotic homologues Phc2 and Phc1 act in synergy to mediate Polycomb-repression of *Hox* genes. *Mol. Cell. Biol.* **25**, 6694-6706.

Kanegae, Y., Lee, G., Sato, Y., Tanaka, M., Nakai, M., Sakaki, T., Sugano, S. and Saito, I. (1995). Efficient gene activation in mammalian cells by using recombinant adenovirus expressing site-specific Cre recombinase. *Nucleic Acids Res.* **23**, 3816-3821.

Kennison, J. A. and Tamkun, J. W. (1988). Dosage-dependent modifiers of Polycomb and antennapedia mutations in Drosophila. *Proc. Natl. Acad. Sci. USA* **85**, 8136-8140.

King, I. F., Francis, N. J. and Kingston, R. E. (2002). Native and recombinant Polycomb group complexes establish a selective block to template accessibility to repress transcription in vitro. *Mol. Cell. Biol.* **22**, 7919-7928.

Lachner, M., O'Sullivan, R. J. and Jenuwein, T. (2003). An epigenetic road map for histone lysine methylation. *J. Cell Sci.* **116**, 2117-2124.

Levine, S. S., Weiss, A., Erdjument-Bromage, H., Shao, Z., Tempst, P. and Kingston, R. E. (2002). The core of the Polycomb repressive complex is compositionally and functionally conserved in flies and humans. *Mol. Cell. Biol.* **22**, 6070-6078.

Milne, T. A., Briggs, S. D., Brock, H. W., Martin, M. E., Gibbs, D., Allis, C. D. and Hess, J. L. (2002). MLL targets SET domain methyltransferase activity to Hox gene promoters. *Mol. Cell* **10**, 1107-1117.

Miyagishima, H., Isono, K., Fujimura, Y., Iyo, M., Takihara, Y., Masumoto, H., Vidal, M. and Koseki, H. (2003). Dissociation of mammalian Polycomb-group proteins, Ring1B and Rae28/Ph1, from the chromatin correlates with configuration changes of the chromatin in mitotic and meiotic prophase. *Histochem. Cell Biol.* **120**, 111-119.

Muller, J., Hart, C. M., Francis, N. J., Vargas, M. L., Sengupta, A., Wild, B., Miller, E. L., O'Connor, M. B., Kingston, R. E. and Simon, J. A. (2002). Histone methyltransferase activity of a Drosophila Polycomb group repressor complex. *Cell* **111**, 197-208.

Nakamura, T., Mori, T., Tada, S., Krajewski, W., Rozovskaia, T., Wassell, R., Dubois, G., Mazo, A., Croce, C. M. and Canaani, E. (2002). ALL-1 is a histone methyltransferase that assembles a supercomplex of proteins involved in transcriptional regulation. *Mol. Cell* **10**, 1119-1128.

Oosterveen, T., Niederreither, K., Dolle, P., Chambon, P., Meijlink, F. and Deschamps, J. (2003). Retinoids regulate the anterior expression boundaries of 5' Hoxb genes in posterior hindbrain. *EMBO J.* **22**, 262-269.

Orlando, V., Strutt, H. and Paro, R. (1997). Analysis of chromatin structure by in vivo formaldehyde cross-linking. *Methods* **11**, 205-214.

Paro, R. (1995). Propagating memory of transcriptional states. *Trends Genet.* **11**, 295-297.

Pasini, D., Bracken, A. P., Jensen, M. R., Denchi, E. L. and Helin, K. (2004). Suz12 is essential for mouse development and for EZH2 histone methyltransferase activity. *EMBO J.* **23**, 4061-4071.

Peters, A. H., Kubicek, S., Mechtler, K., O'Sullivan, R. J., Derijck, A. A., Perez-Burgos, L., Kohlmaier, A., Opravil, S., Tachibana, M., Shinkai, Y. et al. (2003). Dec Partitioning and plasticity of repressive histone methylation states in mammalian chromatin. *Mol. Cell* **12**, 1577-1589.

Pirrotta, V. (1997). PcG complexes and chromatin silencing. *Curr. Opin. Genet. Dev.* **7**, 249-258.

Rastegar, M., Kobrossy, L., Kovacs, E. N., Rambaldi, I. and Featherstone, M. (2004). Sequential histone modifications at Hoxd4 regulatory regions distinguish anterior from posterior embryonic compartments. *Mol. Cell. Biol.* **24**, 8090-8103.

Schoorlemmer, J., Marcos-Gutierrez, C., Were, F., Martinez, R., Garcia, E., Satijn, D. P., Otte, A. P. and Vidal, M. (1997). Ring1A is a transcriptional repressor that interacts with the Polycomb-M33 protein and is expressed at rhombomere boundaries in the mouse hindbrain. *EMBO J.* **16**, 5930-5942.

Shao, Z., Raible, F., Mollaaghababa, R., Guyon, J. R., Wu, C. T., Bender, W. and Kingston, R. E. (1999). Stabilization of chromatin structure by PRC1, a Polycomb complex. *Cell* **98**, 37-46.

Shumacher, A., Faust, C. and Magnuson, T. (1996). Positional cloning of a global regulator of anterior-posterior patterning in mice. *Nature* **383**, 250-253.

Strutt, H. and Paro, R. (1997). The polycomb group protein complex of Drosophila melanogaster has different compositions at different target genes. *Mol. Cell. Biol.* **17**, 6773-6783.

Suzuki, M., Mizutani-Koseki, Y., Fujimura, Y., Miyagishima, H., Kaneko, T., Takada, Y., Akasaka, T., Tanzawa, H., Takihara, Y., Nakano, M. et al. (2002). Involvement of the Polycomb-group gene Ring1B in the specification of the anterior-posterior axis in mice. *Development* **129**, 4171-4183.

Takihara, Y., Tomotsune, D., Shirai, M., Katoh-Fukui, Y., Nishii, K., Motaleb, M. A., Nomura, M., Tsuchiya, R., Fujita, Y., Shibata, Y. et al. (1997). Targeted disruption of the mouse homologue of the Drosophila polyhomeotic gene leads to altered anteroposterior patterning and neural crest defects. *Development* **124**, 3673-3682.

Tamkun, J. W., Deuring, R., Scott, M. P., Kissinger, M., Pattatucci, A. M.,

Kaufman, T. C. and Kennison, J. A. (1992). brahma: a regulator of Drosophila homeotic genes structurally related to the yeast transcriptional activator SNF2/SWI2. *Cell* **68**, 561-572.
van der Lugt, N. M., Alkema, M., Berns, A. and Deschamps, J. (1996). The Polycomb-group homolog Bmi-1 is a regulator of murine Hox gene expression. *Mech. Dev.* **58**, 153-164.
van der Vlag, J. and Otte, A. P. (1999). Transcriptional repression mediated by the human polycomb-group protein EED involves histone deacetylation. *Nat. Genet.* **23**, 474-478.
Vogels, R., Charite, J., de Graaff, W. and Deschamps, J. (1993). Proximal cis-acting elements cooperate to set Hoxb-7 (Hox-2.3) expression boundaries in transgenic mice. *Development* **118**, 71-82.
Voncken, J. W., Roelen, B. A., Roefs, M., de Vries, S., Verhoeven, E., Marino, S., Deschamps, J. and van Lohuizen, M. (2003). Rnf2 (Ring1b) deficiency causes gastrulation arrest and cell cycle inhibition. *Proc. Natl. Acad. Sci. USA* **100**, 2468-2473.
Wang, H., Wang, L., Erdjument-Bromage, H., Vidal, M., Tempst, P., Jones, R. S. and Zhang, Y. (2004a). Role of histone H2A ubiquitination in Polycomb silencing. *Nature* **431**, 873-878.
Wang, L., Brown, J. L., Cao, R., Zhang, Y., Kassis, J. A. and Jones, R. S. (2004b). Hierarchical recruitment of polycomb group silencing complexes. *Mol. Cell* **14**, 637-646.
Yu, B. D., Hanson, R. D., Hess, J. L., Horning, S. E. and Korsmeyer, S. J. (1998). MLL, a mammalian trithorax-group gene, functions as a transcriptional maintenance factor in morphogenesis. *Proc. Natl. Acad. Sci. USA* **95**, 10632-10636.

The EMBO Journal (2006) 25, 3955–3965 | © 2006 European Molecular Biology Organization | All Rights Reserved 0261-4189/06
www.embojournal.org

THE EMBO JOURNAL

Roles of HIPK1 and HIPK2 in AML1- and p300-dependent transcription, hematopoiesis and blood vessel formation

Yukiko Aikawa[1], Lan Anh Nguyen[1], Kyoichi Isono[2], Nobuyuki Takakura[3], Yusuke Tagata[1], M Lienhard Schmitz[4], Haruhiko Koseki[2] and Issay Kitabayashi[1,*]

[1]Molecular Oncology Division, National Cancer Center Research Institute, Chuo-ku, Tokyo, Japan, [2]RIKEN Research Center for Allergy and Immunology, Tsurumi-ku, Yokohama, Japan, [3]Department of Stem Cell Biology, Cancer Research Institute of Kanazawa University, Kanazawa, Japan and [4]Institute for Biochemistry, Medical Faculty, Justus-Liebig-University, Giessen, Germany

Histone acetyltransferases (HATs) p300 and CREB-binding protein (CBP) function as co-activators for a variety of sequence-specific transcription factors, including AML1. Here, we report that homeodomain-interacting protein kinase-2 (HIPK2) forms a complex with AML1 and p300, and phosphorylates both AML1 and p300 to stimulate transcription activation as well as HAT activities. Phosphorylation of p300 is triggered by phosphorylated AML1 as well as by PU.1, c-MYB, c-JUN and c-FOS, and is inhibited by dominant-negative HIPK2. Phosphorylation of p300 and AML1 is impaired in *Hipk1/2* double-deficient mouse embryos. Double-deficient mice exhibit defects in primitive/definitive hematopoiesis, vasculogenesis, angiogenesis and neural tube closure. These phenotypes are in part similar to those observed in p300- and CBP-deficient mice. HIPK2 also phosphorylates another co-activator, MOZ, in an AML1-dependent manner. We discuss a possible mechanism by which transcription factors could regulate local histone acetylation and transcription of their target genes.

The EMBO Journal (2006) 25, 3955–3965. doi:10.1038/sj.emboj.7601273; Published online 17 August 2006
Subject Categories: chromatin & transcription
Keywords: histone acetyltransferase; protein phosphorylation; transcription regulation

Introduction

Covalent modification of histones (acetylation, phosphorylation, methylation, ubiquitination and sumoylation) is essential for regulating gene expression. These modifications appear to be inter-dependent and represent an evolutionarily conserved 'histone code' that alters the interactions between histones and DNA, as well as marks binding sites on histones for effector proteins that regulate gene expression (Jenuwein and Allis, 2001). Histone acetylation is regulated by histone acetyltransferases (HATs) and histone deacetylases (HDACs). HATs and HDACs, directly or through binding to transcription cofactors, interact with transcription factors, which recognize specific DNA sequences in their target genes, to regulate the acetylation of local histones (Marmorstein and Roth, 2001; Thiagalingam *et al*, 2003). The HAT p300 and the closely related CREB-binding protein (CBP) have been shown to function as co-activators for a wide variety of transcription factors and to play central roles in transcriptional control in response to a diverse range of physiological stimuli (Legube and Trouche, 2003).

The *AML1* (*RUNX1*) gene is the most frequent target of leukemia-associated chromosome translocations, which are frequently detected in human leukemia (Look, 1997). AML1 protein forms a heterodimer with CBFβ and binds to a specific DNA sequence to regulate the expression of a number of hematopoietic genes (Meyers *et al*, 1993; Ogawa *et al*, 1993). Both AML1 and CBFβ are essential for the development of all definitive hematopoiesis lineages (Okuda *et al*, 1996; Sasaki *et al*, 1996; Wang *et al*, 1996a, b; Niki *et al*, 1997; Okada *et al*, 1998). AML1 forms complexes with PML and HATs, such as p300/CBP and MOZ, to activate transcription (Kitabayashi *et al*, 1998b, 2001; Nguyen *et al*, 2005). AML1 can act synergistically with other transcription factors, such as AP-1 (Cockerill *et al*, 1996), C/EBPα (Zhang *et al*, 1996), c-Myb (Britos-Bray and Friedman, 1997), PU.1 (Petrovick *et al*, 1998) and Ets-1 (Kim *et al*, 1999). Inducible phosphorylation of AML1 is correlated with increased amounts of MOZ in the AML1 complex during differentiation of M1 myeloid cells (Kitabayashi *et al*, 2001), suggesting that phosphorylation of AML1 is important for regulation of AML1 complex formation and transcriptional activation.

Homeodomain-interacting protein kinases (HIPKs) are nuclear serine/threonine kinases, and three members of the HIPK family (HIPK1, HIPK2 and HIPK3) have been reported (Kim *et al*, 1998). The functional importance of HIPKs has chiefly been studied using HIPK2 and estimated by means of their interacting proteins and phosphorylation targets, including homeoproteins, p53, CtBP1 and Myb (Kim *et al*, 1998; Choi *et al*, 1999; D'Orazi *et al*, 2002; Hofmann *et al*, 2002; Zhang *et al*, 2003; Kanei-Ishii *et al*, 2004). All of these factors represent critical regulators of transcription, suggesting that HIPKs play critical roles in transcriptional regulation.

The activity of CBP or p300 HAT has been shown to be stimulated by a variety of sequence-specific transcription factors, such as HNF1α, HNF4, Sp1, Zta, NF-E2, C/EBPs and phosphorylated Elk1 (Chen *et al*, 2001; Soutoglou *et al*, 2001; Kovacs *et al*, 2003; Li *et al*, 2003; Schwartz *et al*, 2003). Through this stimulation, these sequence-specific transcription factors are thought to increase the acetylation of histones at their target promoters. However, the mechanisms

*Corresponding author. Molecular Oncology Division, National Cancer Center Research Institute, 5-1-1 Tsukiji, Chuo-ku, Tokyo 104-0045, Japan. Tel.: +81 3 3547 5274; Fax: +81 3 3542 0688; E-mail: ikitabay@gan2.ncc.go.jp

Received: 1 March 2006; accepted: 18 July 2006; published online: 17 August 2006

regulating the activity of the transcription factor/HAT complexes on their target genes remain unclear. Here, we report that phosphorylation of p300 is induced by phosphorylated (active) AML1 but not by dephosphorylated (inactive) AML1. AML1 interacts with HIPK2 and mediates phosphorylation of p300 to stimulate HAT activity and induction of transcription. HIPK2-dependent phosphorylation of p300 is also induced by other transcription factors, such as PU.1, c-MYB, c-JUN and c-FOS, suggesting that the present novel mechanism of transcriptional regulation is of general relevance. The importance of HIPK1 and HIPK2 for inducible phosphorylation of p300 was revealed in double-deficient mice, which have defective p300 phosphorylation and show in part a similar phenotype to p300- and CBP-deficient mice.

Results

AML1 is phosphorylated at Ser249 and Ser276

Phosphorylation of AML1 is suggested to be important for its function in transcription and cell differentiation. To determine the phosphorylation sites of AML1, a full-length AML1 protein, AML1b, was purified from L-G myeloid cells, in which AML1 is highly phosphorylated. AML1b was then digested with trypsin and subjected to LC/MS/MS analysis. The predicted phosphorylation sites were Ser249 and Ser276. Comparison of these sites and their surrounding sequences among the different species indicated that the phosphorylation sites of AML1 have been evolutionarily conserved (Figure 1A). Mutants in which Ser249 and/or Ser276 were substituted by alanine, migrated faster than wild type (WT) when expressed in L-G cells (Figure 1B). Phosphatase-treated WT AML1b migrated to a similar position as the S249/276A mutant (Figure 1C). These results suggest that Ser249 and Ser276 of AML1 are phosphorylated in L-G cells. Alteration of Ser266, which is specifically phosphorylated by Erk (Tanaka *et al*, 1996), to alanine did not affect migration (Figure 1B).

HIPK2 phosphorylates AML1 at Ser249 and Ser276

It has been reported that AML1b can be phosphorylated by Erk in 3T3 fibroblasts (Tanaka *et al*, 1996). However, treatment of L-G cells with inhibitors of Erk pathways did not affect the phosphorylation of AML1b (Supplementary Figure S1), suggesting the involvement of other kinases in this phosphorylation. We previously purified the AML1b complex from L-G cells (Kitabayashi *et al*, 2001) and identified the serine/threonine kinase HIPK2 as a component of the AML1 complexes (Supplementary Figure S2). Immunoblot analysis confirmed that HIPK2 is present in the purified complex (Figure 1D). To confirm this interaction, 293T cells were transfected with HA-tagged AML1b together with WT or kinase-dead (KD) point mutant FLAG-tagged HIPK2. HIPK2 proteins were immunoprecipitated with anti-FLAG antibodies. On immunoblot analysis, HA-AML1b was co-precipitated with the WT and mutant HIPK2 (Figure 1E).

To determine whether HIPK2 phosphorylates AML1, we tested the phosphorylation of AML1 by HIPK2 *in vivo* and *in vitro*. 293T cells were transfected with WT and mutant AML1 together with HIPK2. Immunoblot analysis demonstrated that co-transfection of HIPK2 leads to retardation of the protein band for WT AML1b (Figure 1F). Note that AML1b phosphorylation levels are low (i.e., its migration is fast) when AML1 is transiently transfected into 293T cells. Substitution of either Ser249 or Ser276 by alanine diminished the changes in band migration caused by HIPK2. In *in vitro* kinase assays, HIPK2 strongly phosphorylated WT AML1 as well as itself (Figure 1G). Mutations in Ser249 and Ser276 strongly inhibited HIPK2-mediated phosphorylation of AML1. These results indicate that HIPK2 is able to phosphorylate AML1 at Ser249 and Ser276.

HIPK2 stimulates cooperation between AML1, MOZ and p300 in transcription activation

In order to clarify the roles of phosphorylation in the function of AML1, we tested the effects of HIPK2 on AML1-mediated transcription. WT/mutant AML1 was co-transfected with p300/MOZ HAT, HIPK2 and MPO-luc or CCP1-luc reporter genes containing AML1-binding sites. As shown in Figure 1H, MOZ and p300 stimulated AML1-dependent transcription, as reported previously (Kitabayashi *et al*, 2001). MOZ-mediated and p300-mediated transcription activation was strongly enhanced by WT HIPK2 and was completely abolished by KD HIPK2, which functions in a dominant-negative manner. These results suggest that HIPK2 plays an important role in AML1-mediated transcription, particularly in its cooperation with MOZ and p300. HIPK2-, MOZ- and p300-induced transcription activation was almost completely abolished by substitution of Ser249 and Ser276 by alanine (S249/276A). In contrast, this activation activity was strongly enhanced when Ser249 and Ser276 were changed to aspartic acid, which mimics phosphorylated amino acids (S249/276D). These results suggest that phosphorylation of Ser249 and Ser276 on AML1 is essential for transcription activation.

Phosphorylation of p300 by activated AML1 and HIPK2

Because the above results suggest that HIPK2 stimulates AML1 cooperation with p300 and MOZ in transcription, we inferred that HIPK2-mediated AML1 phosphorylation stimulates interaction with p300 and/or MOZ. We then tested the effects of HIPK2 on these interactions. Co-immunoprecipitation analysis indicated that co-transfection with WT or KD HIPK2 had no effect on the interaction between AML1 and p300 (Figure 2A). Unexpectedly, however, we observed differences in mobility of the p300 band after transfection with AML1 and HIPK2. As shown in the upper panel of Figure 2A, co-transfection with AML1 resulted in mobility retardation of p300 (lane 2). This shift in mobility was due to phosphorylation, as treatment with phosphatase restored mobility (Figure 2B). A similar shift in mobility was also induced by co-transfection with WT HIPK2 (Figure 2A, lane 3). More importantly, the AML1-induced mobility shift of p300 was completely inhibited by co-transfection with KD HIPK2 (Figure 2A, lane 6). *In vitro* kinase assays revealed direct phosphorylation of p300 by HIPK2 (Figure 2C). These results suggest that AML1 is able to induce HIPK2-mediated phosphorylation of p300.

The mobility shift of p300 was not induced when co-transfection was performed with an alanine mutant (2A = S249/276A), which lacks phosphorylation sites (upper panel in Figure 2D). In contrast, an aspartic acid mutant (2D = S249/276D), which mimics phosphorylated AML1, induced a greater mobility shift than WT AML1. These results suggest that activation of AML1 by phosphorylation is required for AML1-induced phosphorylation of p300. Co-immunoprecipitation experiments indicated that

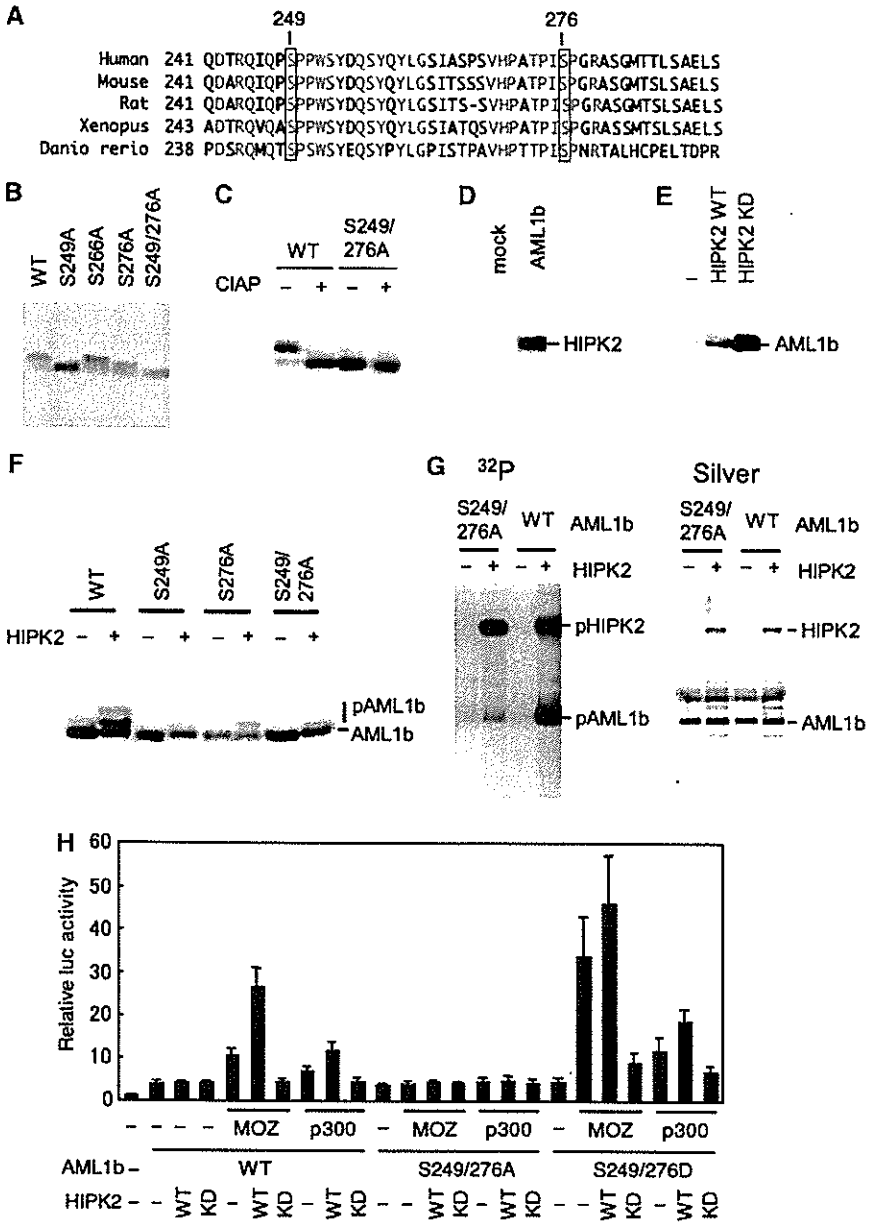

Figure 1 AML1 is phosphorylated at Ser249 and Ser276 by HIPK2. (**A**) Phosphorylation sites are evolutionarily conserved. (**B**) Migration of WT and mutant AML1 in L-G cells. (**C**) Phosphatase treatment of AML1. Purified WT and S249/276A mutant AML1b were treated with (+) or without (−) calf intestine alkaline phosphatase (CIAP) and analyzed by immunobloting with anti-AML1 antibody. (**D**) AML1 complex contains HIPK2. Purified AML1 complexes were analyzed by immunobloting with anti-HIPK2 antibody. (**E**) Interaction of AML1 with HIPK2. 293T cells were transfected with HA-AML1b together with either FLAG-tagged WT or KD HIPK2. Immunoprecipitates with anti-FLAG were analyzed by immunoblotting with anti-HA antibody. (**F**) Phosphorylation of AML1 by HIPK2. Cell extracts from 293T cells expressing WT or mutants of HA-tagged AML1 and HIPK2 were subjected to immunoblot analysis with anti-HA antibody. (**G**) Phosphorylation of AML1 *in vitro*. Purified WT or mutant AML1b proteins were tested for *in vitro* kinase activity. (**H**) HIPK2 activates AML1-mediated transcription. SaOS2 cells were transfected with 50 ng of MPO-luc, 200 ng of LNCX-AML1b, 250 ng of MOZ or p300, 250 ng of WT or KD mutant of HIPK2 and 2 ng of phRL-cmv. Cell lysates were analyzed for luciferase activity at 24 h after transfection.

neither the alanine nor aspartic acid mutation affected the interaction between AML1 and p300 (Figure 2D, lower panel). In addition, neither of these mutations affected the interaction between AML1 and HIPK2 (Supplementary Figure S3).

HIPK2 activates p300

In order to investigate the role of phosphorylation by HIPK2 on p300 function, we tested the effects of HIPK2 on p300 HAT and transcription activation activities. To test HAT activity, FLAG-tagged p300 was co-transfected with WT HIPK2 and KD mutant, purified using anti-FLAG antibodies and tested for HAT activity. Intrinsic HAT activity of p300 was activated by WT HIPK2 and AML1b, and was inhibited by KD HIPK2 (Figure 2E). Reporter analysis indicated that WT HIPK2 and AML1 stimulated transcription activation by Gal4-p300 (Figure 2F). These results suggest that HIPK2 stimulates HAT activity and p300-mediated transcription activation.

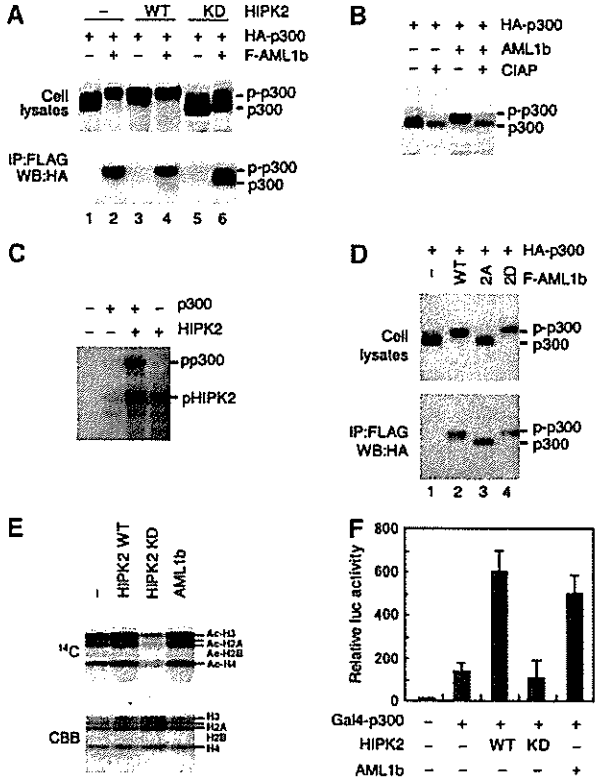

Figure 2 HIPK2 mediates AML1-dependent phosphorylation of p300. (A) AML1 induces phosphorylation of p300. 293T cells were transfected with FLAG-AML1b, HA-p300 and HIPK2. Cell lysates were immunoprecipitated with anti-FLAG antibodies. Cell lysates (1%) and immunoprecipitates were then analyzed by immunoblotting with anti-HA antibody. (B) CIAP-treatment of AML1–p300 complex. 293T cells were transfected with HA-p300 and FLAG-AML1b. After immunoprecipitation with anti-HA antibodies, immunoprecipitates were treated with CIAP and analyzed by immunoblotting with anti-HA antibody. (C) Phosphorylation of p300 *in vitro*. Purified WT p300 protein was incubated with or without HIPK2 in the presence of [γ^{32}P]ATP and was separated by 7% SDS–PAGE. Gels were dried and subjected to autoradiography. (D) Phosphorylation of AML1 is required for AML1-induced phosphorylation of p300. 293T cells were transfected with HA-p300 and FLAG-tagged WT, S249/276A (2A) or S249/276A (2D) mutant AML1b. After immunoprecipitation with anti-FLAG antibodies, cell lysates (1%) and immunoprecipitates were analyzed by immunoblotting with anti-HA antibody. (E) HIPK2 and AML1 stimulates HAT activity of p300. 293T cells were transfected with FLAG-p300 together with either WT or KD HIPK2, or AML1b. After immunoprecipitation with anti-FLAG antibodies, immunoprecipitates were analyzed for HAT activity. (F) HIPK2 and AML1 stimulate transcription activation by a Gal4-p300 fusion protein. 293T cells were transfected with 500 ng of pFR-luc(Gal4-luc), 100 ng of Gal4-p300, 400 ng of WT or KD HIPK2, or AML1b and 2 ng of phRL-cmv. Cell lysates were analyzed for luciferase activity at 24 h after transfection.

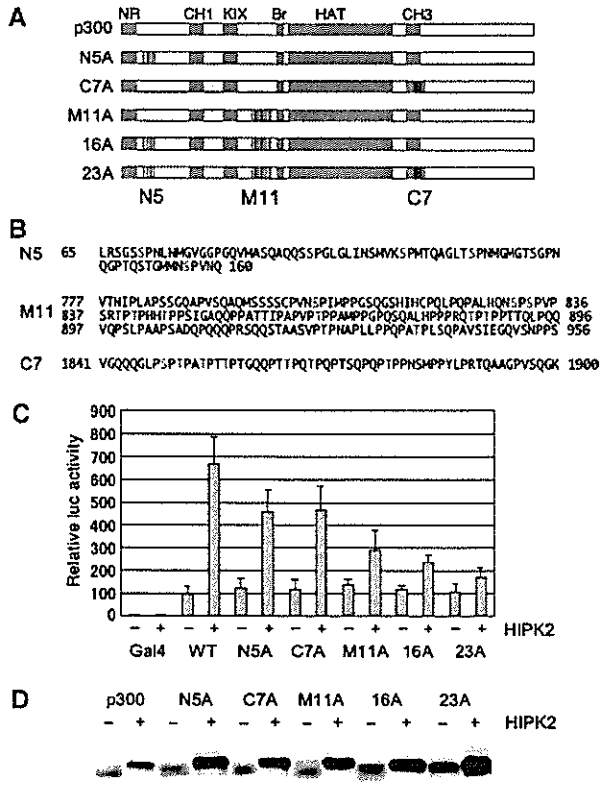

Figure 3 Phosphorylation sites of p300 by HIPK2. (A) Schematic representation of p300 mutants used for determining HIPK2-induced phosphorylation sites. (B) Amino-acid sequence of putative HIPK2 phosphorylation sites of p300. Serines or threonines shown in red were substituted with alanines. (C) HIPK2-induced activation of transcription by Gal4-p300 mutants. 293T cells were transfected with 500 ng of pFR-luc(Gal4-luc), 100 ng of WT or mutant Gal4-p300, 400 ng of HIPK2 and 2 ng of phRL-cmv. Cell lysates were prepared at 24 h after transfection and were analyzed for luciferase activity. (D) Phosphorylation of p300 mutants by HIPK2. 293T cells were transfected with WT or mutants of Gal4-p300 together with HIPK2. Cell lysates were subjected to immunoblot analysis with anti-Gal4 antibody.

The p300 sites phosphorylated by HIPK2 were investigated using various mutants of Gal4-p300, in which the putative phosphorylation sites (SP and TP) were substituted with AP, and these mutants were tested for both transcription activation and phosphorylation by HIPK2. Transcription activation and phosphorylation of p300 were markedly reduced by substitution of the 23 SP/TP sites (Figure 3).

Interaction between HIPK2 and p300

Overexpressed HIPK2 was able to phosphorylate p300, even in the absence of AML1, thus suggesting a physical interaction between HIPK2 and p300. To test this interaction, FLAG-tagged HIPK2 or AML1 were co-transfected with HA-p300 or truncated versions thereof as schematically shown in Figure 4A. On IP-Western analysis, p300 was co-precipitated with WT and KD HIPK2 in addition to AML1 (Figure 4B). Reciprocal co-immunoprecipitation experiments also indicated that WT and KD HIPK2 were co-precipitated with p300 (Figure 4C). Deletion analysis of p300 allowed mapping of the HIPK2-binding domain (1304–1571) and AML1-binding domain (142–597) (Figure 4D). Interactions between AML1 and p300 were markedly reduced by deletion of the 142–957 region of p300, but the interaction could be still detected weakly after overexposure (Figure 4D), suggesting an indirect interaction through other factors or another AML1-interacting domain. GST pull-down analysis indicated that HIPK2, which was translated *in vitro*, bound to bacterially produced GST-AML1b and GST-p300(HAT) proteins (Figure 4E), suggesting that HIPK2 directly interacts with AML1 and p300.

Phosphorylation of p300 by various transcription factors

Various transcription factors are known to utilize p300 as a co-activator. It was recently reported that the C/EBP family of

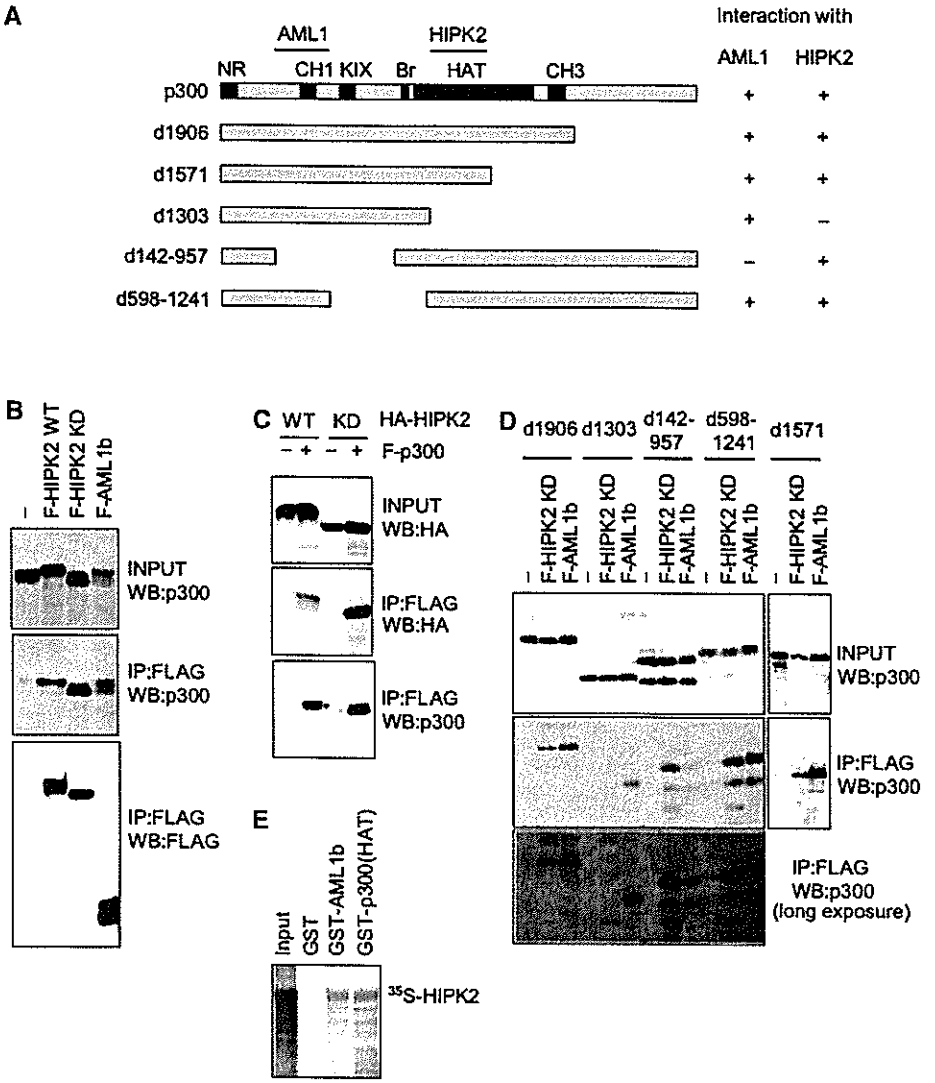

Figure 4 Interaction of p300 and HIPK2. (A) Schematic representation of p300 deletion mutants used for determining HIPK2-binding domains. (B) Interaction of p300 with HIPK2. 293T cells were transfected with p300 together with FLAG-tagged WT or KD HIPK2, or AML1b. (B–D) Cell lysates (1%) and immunoprecipitates with anti-FLAG antibodies were analyzed by immunoblotting with anti-p300, anti-HA or anti-FLAG antibodies. (C) Reciprocal coimmunoprecipitation of HIPK2 and p300. (D) Interaction of p300 mutants with HIPK2 and AML1. 293T cells were transfected with p300 mutants as shown together with KD HIPK2 or AML1b. The lower panel represents a longer exposure of the same membrane shown in the middle panel. (E) HIPK2 translated *in vitro* and labelled with ^{35}S was tested for binding to bacterially produced GST, GST-AML1b and GST-p300(HAT) proteins as shown. The input lane represents 10% of the material used for binding to the GST fusion protein.

transcription factors induce phosphorylation of p300 and CBP (Kovacs *et al*, 2003; Schwartz *et al*, 2003). To test whether phosphorylation of p300 is induced by other transcription factors that bind to p300, several transcription factors were co-transfected with p300. Mobility shifts of p300 were induced by AML/runx family members, PU.1, C/EBPα, C/EBPε, c-MYB, c-JUN and c-FOS, but were not induced by IRF3, p53, RARα or ATF2 (Figures 5A and C). To determine whether these shifts were mediated by HIPK2, the dominant-negative HIPK2 was co-transfected with these factors. As shown in Figure 5B, the dominant-negative HIPK2 completely inhibited the phosphorylation of p300 induced by AML1/2/3, PU.1, c-MYB, c-JUN and c-FOS, which suggests that HIPK2 mediates p300 phosphorylation by these factors. On the other hand, phosphorylation induced by C/EBPα and C/EBPε was only partially inhibited by the dominant-negative HIPK2, which suggests that other kinase(s) are involved (Figure 5C).

Roles of HIPK family members in phosphorylation and transcription

We generated *Hipk1*- and *Hipk2*-deficient mice by targeted disruption of the corresponding genes (Isono *et al*, 2006). *Hipk1* and *Hipk2* single-deficient mice are grossly normal (Kondo *et al*, 2003; Wiggins *et al*, 2004), but *Hipk1/Hipk2* double homozygotes die between E9.5 and E12.5 (Isono *et al*, 2006). These findings suggest functional redundancy between HIPK1 and HIPK2. We thus addressed the physiological roles of HIPK family proteins by using *Hipk1/Hipk2* double mutants. To investigate the phosphorylation of p300, proteins were extracted from whole embryos at E10.0 and were analyzed by immunoblottng with anti-p300 antibodies. Although significant amounts of highly phosphorylated forms of p300 were observed in *Hipk1*-deficient, *Hipk2*-deficient and WT embryos, highly phosphorylated forms were severely reduced in *Hipk1/Hipk2* double-deficient

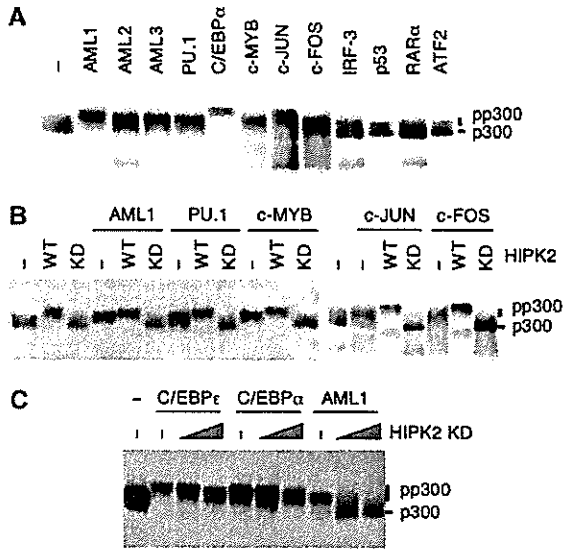

Figure 5 HIPK2 mediates phosphorylation of p300 induced by a set of transcription factors. (A) Phosphorylation of p300 by various transcription factors. 293T cells were transfected with HA-p300 together with various transcription factors. Cell lysates were subjected to immunoblot analysis with anti-HA antibody. (B) Effects of WT and KD HIPK2 on transcription factor-induced phosphorylation of p300. 293T cells were transfected with HA-p300 and the transcription factors indicated together with WT and KD HIPK2. (C) Effects of KD HIPK2 on phosphorylation of p300. 293T cells were transfected with HA-p300 (0.2 μg) and either C/EBPε, C/EBPα or AML1b (0.4 μg) together with increasing amounts (0.2 and 0.4 μg) of KD HIPK2.

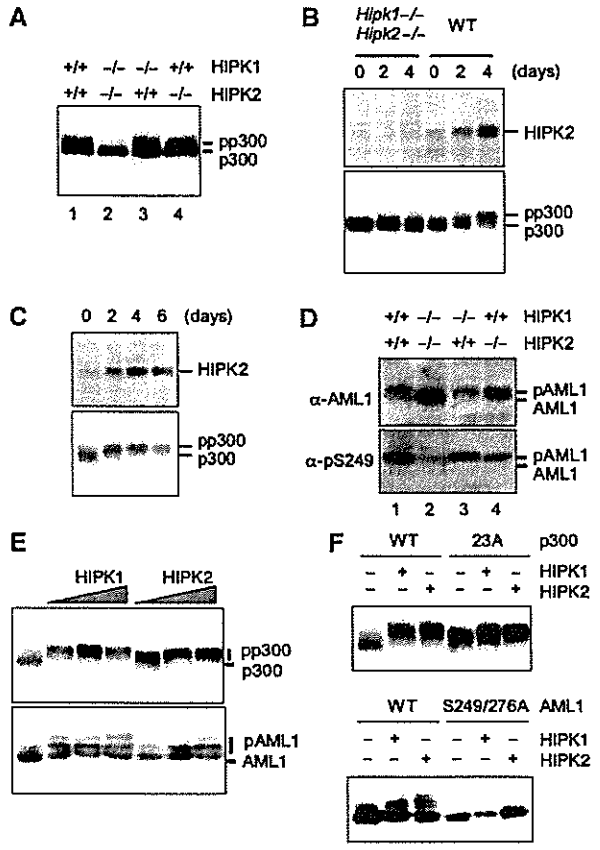

Figure 6 HIPK1 and HIPK2 are essential for phosphorylation of p300 and AML1. (A) Phosphorylation of p300 in HIPK1- and/or HIPK2-deficient embryos. Proteins were extracted from WT and mutant E10.0 embryos and were subjected to immunoblot analysis with anti-p300 antibody. (B) Expression of HIPK2 and phosphorylation of p300 during differentiation of ES cells. WT and Hipk1/2 double-deficient ES cells were exposed to 1 μM retinoic acid for 2 and 4 days. The cell lysates were subjected to immunoblot analysis with anti-HIPK2 and anti-p300 antibodies. (C) Expression of HIPK2 and phosphorylation of p300 during differentiation of myeloid cells. 32Dcl3 cells were exposed to 10 ng G-CSF for indicated number of days. (D) Phosphorylation of AML1 in HIPK1- and/or HIPK2-deficient yolk sac. Yolk sac cells from E10.0 embryos were cultured on OP9 cells for 5 days. Cell lysates were subjected to immunoblot analysis with anti-AML1 and phospho-S249-specific AML1 antibodies. (E) Phosphorylation of p300 and AML1 by HIPK1 and HIPK2. 293T cells were transfected with HA-p300 or AML1 (0.2 μg) together with increasing amounts (0.05, 0.1, 0.2 μg) of HIPK1 or HIPK2. Cell lysates were subjected to immunoblot analysis with anti-HA antibody. (F) 293T cells were transfected with WT or mutant Gal4-p300 or HA-AML1 together with HIPK1 or HIPK2. Cell lysates were subjected to immunoblot analysis with anti-Gal4 or anti-HA antibody.

embryos (Figure 6A). It has been reported that phosphorylation of p300 is stimulated during retinoic acid-induced differentiation of embryonic stem (ES) cells (Kitabayashi *et al*, 1995). To test whether HIPK1 and HIPK2 are required for p300 phosphorylation, we investigated changes in phosphorylation of p300 after retinoic acid-induced differentiation of WT and HIPK1/HIPK2 double knockout ES cells. Phosphorylation of p300 was stimulated and was associated with expression of HIPK2 during differentiation of WT ES cells but not in double knockout ES cells (Figure 6B). Induction of p300 phosphorylation and HIPK2 expression was also observed in G-CSF-induced differentiation of 32Dcl3 cells (Figure 6C).

To confirm the phosphorylation of AML1, which is predominantly expressed in hematopoietic cells, nonadherent cells were prepared from the yolk sac of mutant embryos and were expanded by culture *in vitro* for 5 days. Immunoblot analysis using anti-AML1 antibody indicated that hypophosphorylated forms of AML1 were increased in *Hipk1/Hipk2* double-deficient cells when compared with those in single-deficient cells or WT cells. Immunoblot analysis using phospho-specific antibody (Supplementary Figure S4), which detects AML1 phosphorylated at Ser249, indicated that phosphorylated AML1 was markedly decreased in *Hipk1/Hipk2* double-deficient cells (Figure 6D).

In order to test whether HIPK1 can induce phosphorylation of p300 and AML1, 293T cells were transfected with p300 and AML1 together with HIPK1. Phosphorylation of p300 and AML1 was strongly induced by HIPK1 as well as by HIPK2 (Figure 6E). These phosphorylations were largely inhibited by substitution with alanine at the phosphorylation sites (Figure 6F). Co-immunoprecipitation analysis indicated that HIPK1 as well as HIPK2 interact with AML1 (Supplementary Figure S5).

Reporter analysis indicated that HIPK1 also stimulates transcription activation by Gal4-p300 and by AML1 (Figure 7A and B). Reporter analysis using WT and HIPK1/2 double-deficient mouse embryonic fibroblasts showed an impaired AML1-dependent transcription in HIPK1/HIPK2 double-deficient cells (Figure 7C). Thus, we conclude that both HIPK1 and HIPK2 mediate the phosphorylation of p300 and AML1, and enhance AML1- and p300-dependent transcription.

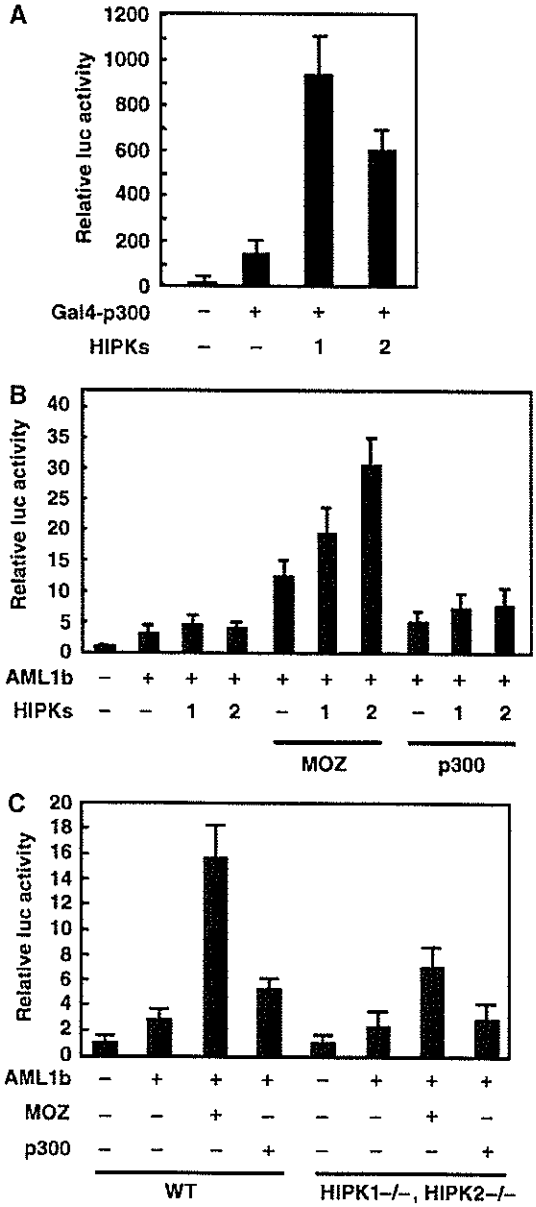

Figure 7 HIPK1 and HIPK2 are involved in p300- and AML1-mediated transcription. (A) 293T cells were transfected with 500 ng of pFR-luc(Gal4-luc), 100 ng of Gal4-p300, 400 ng of HIPK1 or HIPK2, and 2 ng of phRL-cmv. (B) SaOS2 cells were transfected with 50 ng of MPO-luc, 200 ng of LNCX-AML1b, 250 ng of MOZ or p300, 250 ng of HIPK1 or HIPK2, and 2 ng of phRL-cmv. (C) WT and HIPK1/2 double-deficient MEFs were transfected with 50 ng of MPO-luc, 200 ng of LNCX-AML1b, 500 ng of MOZ or p300, and 2 ng of phRL-cmv. Cell lysates were analyzed for luciferase activity at 24 h after transfection.

Hematopoiesis defects in HIPK1/2-deficient mice

Because AML1, p300 and the closely related CBP are essential for hematopoiesis (Okuda *et al*, 1996; Wang *et al*, 1996a; Oike *et al*, 1999; Tanaka *et al*, 2000; Kasper *et al*, 2002; Rebel *et al*, 2002), we analyzed hematopoietic cells in the yolk sac and the paraaortic splanchnopleural (P-Sp) region, in which definitive hematopoiesis is first detected during development. A marked decrease in the total number of cells was observed in *Hipk1−/−Hipk2−/−* yolk sacs (Figure 8A). To investigate

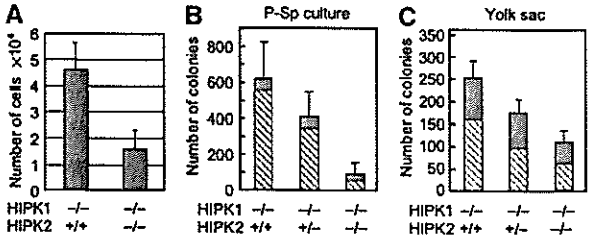

Figure 8 Hematopoiesis in HIPK1/2 mutant embryos. (A) Yolk sac cells from embryos at E9.5 were dispersed into single-cell suspensions and the numbers of nucleated erythroid cells were counted. (B) Colony-forming cells in P-Sp cultures. P-Sp explants derived from E9.5 embryos obtained by intercrossing HIPK1−/−,HIPK2+/− mice were cultured on OP9 stromal cells for 7 days and were subjected to colony-formation assay. Dot-filled and oblique-line-filled boxes represent the number of erythroid and myeloid colonies, respectively. (C) Colony-forming cells in yolk sac. Yolk sac cells were directly subjected to colony-formation assay.

definitive hematopoiesis, *Hipk1−/−Hipk2+/−* mice were mated, and the P-Sp region of embryos at 9.5-dpc were dissected and cultured on OP9 cells. After 7 days of culture, colony-forming cells (CFCs) from nonadherent cells were examined on methylcellulose medium. Yolk sac cells were directly tested for CFCs. As shown in Figure 8B and C, the total number of CFCs in the yolk sac and cultured P-Sp cells from double-deficient (*Hipk1−/−Hipk2−/−*) mutants was markedly reduced when compared with those from control littermates (*Hipk1−/−Hipk2+/−* or *Hipk1−/−Hipk2+/+*). These results suggest that primitive as well as definitive hematopoiesis is defective in *Hipk1/Hipk2* double-deficient embryos.

Defects in vasculogenesis/angiogenesis in HIPK1/2-deficient mice

Morphologic evaluation of embryos revealed severe defects in vessel formation in *Hipk1/Hipk2* double-homozygous mutant embryos and yolk sacs at E10.0 (Figure 9A and B). Similar defects in vessel formation are also observed in *p300*- and *cbp*-deficient mice (Yao *et al*, 1998; Oike *et al*, 1999; Tanaka *et al*, 2000). To further study the vascular system, whole embryos were stained with anti-PECAM-1 monoclonal antibody, which detects differentiated endothelial cells. *Hipk1/Hipk2* double-deficient embryos failed to form an organized vascular network (Figure 9C). Gross defects in vascular branching were observed, particularly in the head and trunk (Figure 9D and E). To further investigate the defects in the vascular networks in *Hipk1/Hipk2* double mutant embryos, P-Sp regions were dissected from E8.75 embryos obtained by intercrossing *Hipk1−/−Hipk2+/−* mutant mice, cultured on OP9 stromal cells, and stained with anti-PECAM-1 antibody (Figure 9F). Both sheet (Figure 9G) and network (Figure 9H) formations, which are indicative of vasculogenesis and angiogenesis, respectively, were severely affected in P-Sp cultures from *Hipk1/Hipk2* double-homozygous mutant embryos, while cultures from littermate embryos developed normally. The double-homozygous mutant embryos at E8.75 were comparable in size to their littermates (data not shown). Thus, we concluded that vascular formation in *Hipk1/Hipk2* double-homozygotes is impaired rather than delayed.

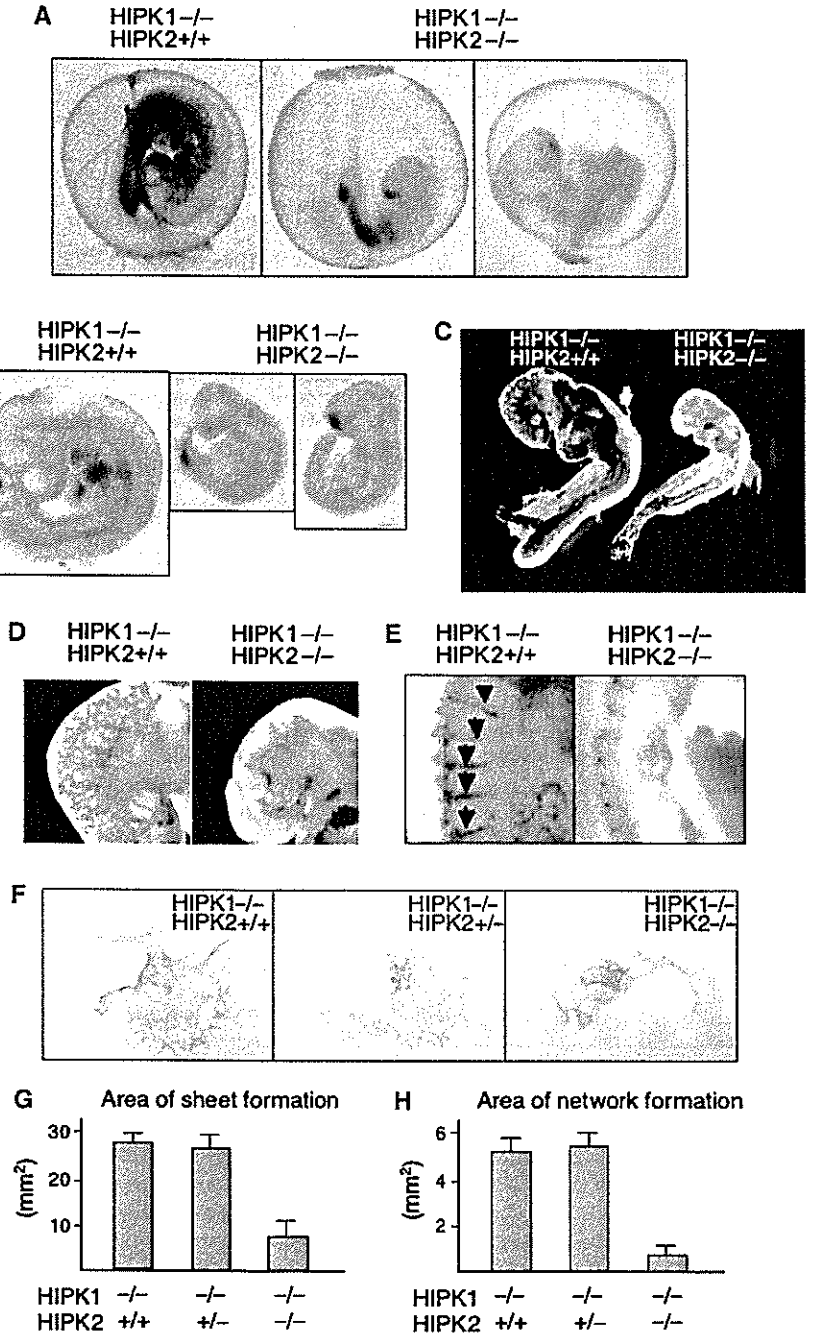

Figure 9 HIPK1/2 mutant embryos showed defective vasculogenesis and angiogenesis. (A, B) Phenotypic comparison of E10.0 *Hipk1−/−*, *Hipk2+/+* and *Hipk1−/−,Hipk2−/−* embryos with (A) and without (B) yolk sac. (C) Whole-mount immunohistostaining with anti-CD31 (PECAM-1) mAb of E9.5 *Hipk1−/−,Hipk2+/+* and *Hipk1−/−,Hipk2−/−* embryos. (D) Primary vascular plexus observed in mutant heads. (E) Migration of endothelial cells forming intersomitic vessels. (F–H) Vasculo-angiogenesis in P-Sp culture. P-Sp explants derived from E8.75 embryos obtained by intercrossing *Hipk1−/−,Hipk2+/−* mice were cultured on OP9 stromal cells and were stained with anti-CD31 mAb. Representative results are shown in (F). The average values of areas of vascular sheet formation and vascular network formation are shown in (G) and (H), respectively.

Discussion

AML1 stimulates HIPK2-mediated phosphorylation of p300 and activates transcription

In the present study, we found that co-expression of AML1 induced phosphorylation of p300. This effect was inhibited by the dominant-negative form of HIPK2 and was enhanced by WT HIPK2. These results suggest that HIPK2 mediates the AML1-induced phosphorylation of p300. HIPK2-mediated phosphorylation of p300 stimulates its HAT activity and activates p300-dependent transcription. AML1 interacts with both p300 and HIPK2, and thus AML1 induces phosphorylation of p300 by stimulating the physical interaction between the enzyme HIPK2 and the substrate p300.

Interestingly, the alanine mutant AML1-S249/276A, which lacks phosphorylation sites, did not induce p300 phosphorylation, while the aspartic acid mutant AML1-S246/276D, which mimicks the phosphorylated form, induced phosphorylation of p300 more efficiently than WT AML1. Moreover, AML1/p300-mediated transcriptional activation was inhibited by alanine mutations and enhanced by aspartic acid mutations on the phosphorylation sites of AML1. These findings suggest that phosphorylation of AML1 is required for the HIPK2-mediated phosphorylation of p300 and subsequent transcription activation. Thus, AML1 not only recruits HIPK2 to the substrate p300 but also functions as a regulatory subunit for HIPK2 to control p300 phosphorylation, local histone acetylation and transcription of target genes.

HIPK-induced phosphorylation of p300 is common to regulation by various transcription factors

Phosphorylation of p300 was also induced by transcription factors such as the AML1/runx family members, PU.1, c-MYB, c-JUN and c-FOS. These effects were inhibited by co-expression of dominant-negative HIPK2, suggesting that HIPK family members are involved in the phosphorylation of p300 by these transcription factors. It is likely that these transcription factors also regulate transcription by recruiting HIPKs and inducing p300 phosphorylation on their target genes in the same way as AML1. Thus, HIPK-mediated phosphorylation of p300 is a common event in transcriptional regulation by a range of transcription factors. Phosphorylation of p300 was not induced by transcription factors such as IRF3, p53, RARα and ATF2 under the conditions tested, although these transcription factors were able to interact with p300. As these factors are activated in response to a range of physiological stimuli, it is possible that additional modifications or factors induced by these stimuli are required for p300 phosphorylation.

Highly phosphorylated forms of p300 were scarcely detected in *Hipk1/2* double-deficient embryos, suggesting that phosphorylation of p300 is largely regulated by HIPK1 and HIPK2 during embryonic development. A variety of transcription factors, including jun, fos, runx and ets family members, are probably involved in the regulation of p300 phosphorylation during embryogenesis and hematopoiesis. It has been reported that phosphorylation of p300 is stimulated and is associated with expression of c-JUN during retinoic acid-induced differentiation of F9 embryonic carcinoma cells and ES cells (Kitabayashi *et al*, 1995). We found here that the induction of p300 phosphorylation was inhibited in *Hipk1/2* double-deficient ES cells. Thus, the phosphorylation of p300 in this process is likely to be mediated by HIPK1 and/or HIPK2 in combination with transcription factors, including c-JUN.

It has been reported that AML1 activates transcription synergistically with other transcription factors, such as AP-1 (jun/fos), C/EBPα, c-Myb, PU.1 and Ets-1, to activate transcription (Cockerill *et al*, 1996; Zhang *et al*, 1996; Britos-Bray and Friedman, 1997; Petrovick *et al*, 1998; Kim *et al*, 1999). We found here that phosphorylation of p300 is a common effect induced by these transcription factors, thus suggesting that phosphorylated forms of p300 and HIPK2 are involved in the above-mentioned synergistic effects.

Role of phosphorylation in p300/CBP function

HIPK1 and HIPK2 double-deficient embryos died between E9.5 and E12.5 and exhibited defects in vasculogenesis, angiogenesis, and primitive and definitive hematopoiesis. The double homozygous mutants exhibited developmental retardation and failed to close the anterior neuropore (Isono *et al*, 2006). These phenotypes were in part similar to those observed in p300- and CBP-deficient mice. Both p300- and CBP-deficient mice show embryonic lethality and die between E9.5 and E12.5 (Yao *et al*, 1998; Oike *et al*, 1999; Tanaka *et al*, 2000). Moreover, double heterozygosity for *p300* and *cbp* is invariably associated with embryonic death, suggesting the overlapping function and overall gene dosage requirement of p300 and CBP. *p300*- and *cbp*-deficient embryos exhibited defective blood vessel formation, defective neural tube closure and apparent developmental retardation, as well as defects in both primitive and definitive hematopoiesis. Phosphorylation of p300 was inhibited in *Hipk1/Hipk2*-double deficient embryos. Taken together these findings suggest that phosphorylation of p300/CBP by HIPK1/HIPK2 is essential for p300 and CBP function in embryonic development. However, we cannot exclude a possibility that HIPK1/HIPK2 may have other substrates whose phosphorylation is required for hematopoiesis and development. p300 null embryos show other defects, in addition to those found in *Hipk1/Hipk2*-double deficient embryos, including anomalous heart formation, turning of the embryo and edema formation (Yao *et al*, 1998). That these defects are not observed in *Hipk1/Hipk2*-double deficient embryos suggests that some of the function of p300 is independent of HIPK1/2-mediated phosphorylation.

HIPK2 regulates transcription via multiple factors

We also found that co-expression of AML1 and HIPK2 induced phosphorylation of MOZ (Supplementary Figure S6). The phosphorylation of MOZ was not efficiently induced by either AML1 or HIPK2 alone, and thus interaction between these three molecules is likely to be required for efficient MOZ phosphorylation. AML1 probably stimulates MOZ phosphorylation by accelerating the physical interaction between HIPK2 and MOZ. Moreover, a highly phosphorylated form of MOZ was preferentially co-precipitated with AML1, suggesting that AML1 interacts with the highly phosphorylated form of MOZ more strongly than with the hypophosphorylated form. Thus, HIPK2 stabilizes the AML1/MOZ complex by phosphorylating MOZ. We generated MOZ mutant mice and found that MOZ homozygous mutant mice die around E15.5 and exhibit severe defects in definitive hematopoiesis (Katsumoto *et al*, 2006). *Hipk1/Hipk2*-deficient mice also show defective definitive hematopoiesis. These defects appear to be more severe than those observed in *cbp*- or *p300*-deficient mice. This is probably due to reduced MOZ activity, in addition to inactive AML1 and p300/CBP, in *Hipk1/Hipk2*-deficient mice.

It was recently reported that the Groucho corepressor is phosphorylated by *Drosophila* HIPK2 and subsequently dissociates from the corepressor complex (Choi *et al*, 2005). TLE, the human homolog of Groucho, also reportedly interacts with AML1 and suppresses AML1-induced transactivation (Imai *et al*, 1998; Levanon *et al*, 1998). Taken together with these findings, the present results suggest that HIPKs play a key role in regulating the transcription of target genes

by relieving Groucho-mediated transcriptional repression as well as by activating transcription factor/HAT complexes.

Materials and methods

Cells and retroviruses

Culture of L-G, BOSC23 and SaOS2 cells were performed as described previously (Kitabayashi *et al*, 2001). Retrovirus infection of cells was performed as described previously (Kitabayashi *et al*, 1998a).

Plasmids

The AML1 expression vectors pLNCX-FLAG-AML1a, pLNCX-FLAG-AML1b, pLNCX-HA-p300, pLNCX-HA-MOZ, mCCP1-luc and MPO-luc were as described previously (Kitabayashi *et al*, 2001). LNCX-FLAG-HIPK2 and LNCX-HA-HIPK2 were generated by subcloning WT and KD HIPK2 (Hofmann *et al*, 2002) into a retrovirus-derived LNCX vector. CMV-HIPK1 was as described by Isono *et al* (2006).

Mass spectrometry

AML1 proteins were purified from L-G cells, digested with trypsin and subjected to LC/MS/MS analysis as described previously (Kitabayashi *et al*, 2001). Phosphopeptides were identified using TurboSEQUEST software.

Immunoprecipitation, immunoblotting and antibodies

Immunoprecipitation and immunoblotting analyses were performed as described previously (Kitabayashi *et al*, 2001). The following primary antibodies were used in the present study: anti-FLAG (M2) antibody (Sigma), anti-HA (3F10) antibody (Roche), anti-AML1 antibody (Kitabayashi *et al*, 1998a), anti-HIPK2 antibody (Hofmann *et al*, 2002) and anti-p300 antibody (N15) (Santa Cruz). The anti-phospho-S249 AML1 antibody was generated by immunizing rabbits with phosphopeptides RQIQPpSPPWSY corresponding to residues 244-254 of human AML1b.

HAT activity and kinase activity in vitro

For HAT activity, 293 cells were transfected with FLAG-tagged p300 together with WT or KD HIPK2. FLAG-p300 was purified by immunoprecipitation as described above and incubated in a 10-μl volume containing 50 mM Tris (pH 8.0), 10% glycerol, 1 mM DTT, 1 mM PMSF, 10 mM sodium butyrate, 0.5 μl of [1-^{14}C]-acetyl-CoA (50 μCi/ml, Amersham), and 0.5 μg each of histones H2A, H2B, H3 and H4 at 37°C for 1 h. Reaction mixtures were analyzed by 18% SDS–PAGE, and gels were subjected to autoradiography. Histone acetylation was measured using a BAS2000 imaging analyzer (Fuji).

For kinase activity, FLAG-tagged WT and mutant AML1b, WT HIPK2 and p300 were purified by immunoprecipitation, as described above, and were incubated in 20 mM Tris–Cl (pH 7.5), 10 mM $MgCl_2$, 1 mM DTT, and 50 μM ATP, 5 μCi [γ-^{32}P]-ATP at 37°C for 30 min. Reaction mixtures were analyzed by SDS–PAGE, and gels were subjected to autoradiography.

Luciferase assay

Reporter analysis was performed as described previously (Kitabayashi *et al*, 2001).

GST pull-down assay

The GST pull-down assay was performed as described previously (Hofmann *et al*, 2002). GST-AML1b has been described previously (Kitabayashi *et al*, 1998b). GST-p300(HAT) was generated by subcloning of an *Eco*RI–*Stu*I fragment into pGEX.

In vitro culture of P-Sp

P-Sp culture conditions were as described (Takakura *et al*, 2000).

In vitro hematopoietic colony assays

P-Sp cultures from mouse embryos were dispersed into single-cell suspensions and cultured on 1% methylcellulose in Iscove's modified Dulbecco's medium (IMDM) containing 15% fetal bovine serum, 1% bovine serum albumin, 10 μg/ml rh insulin, 200 μg/ml human transferrin, 100 μM 2-mercaptoethanol, 2 mM L-glutamine, 50 ng/ml rm SCF, 10 ng/ml rmIL-3, 10 ng/ml rh IL-6 and 3 U/ml erythropoietin (MethoCult GF M3434) (Stem Cell Technology Inc., Vancouver, Canada). Cultures were maintained at 37°C under humidified conditions with 5% CO_2. Colonies containing more than 50 cells were counted on day 12, and myeloid CFUs, erythroid burst forming units (BFU-E) and CFU-Mix were defined based on morphology.

Isolation and differentiation of ES cells

Hipk1−/−Hipk2+/− mice were mated and blastocysts were harvested on day E3.5 then individually cultured in ES cell medium (containing 20% fetal calf serum and leukemia inhibitory factor (LIF)) on a feeder layer of mitomycin C-treated embryonic fibroblasts, as previously described (Auerbach *et al*, 2000). ES cells were cultured in ES cell medium containing 10% fetal calf serum plus LIF. Cells were then plated on gelatinized 100-mm plates at a density of 1×10^6 cells/plate in the absence of LIF for 24 h, and then they were treated with 1 μM RA for various periods of time.

Supplementary data

Supplementary data are available at *The EMBO Journal* Online (http://www.embojournal.org).

Acknowledgements

We would like to thank Dr M Kurokawa and Dr M Nakagawa for their advice on preparation of hematopoietic cells in the P-Sp culture, Dr T Nakano for supplying the OP9 cells, and Ms N Aikawa and Ms M Shino for technical assistance. This work was supported in part by Grants-in-Aid for Scientific Research from the Ministry of Health, Labor and Welfare and from the Ministry of Education, Culture, Sports, Science and Technology, and by the Program for Promotion of Fundamental Studies from the National Institute of Biomedical Innovation of Japan.

References

Auerbach W, Dunmore JH, Fairchild-Huntress V, Fang Q, Auerbach AB, Huszar D, Joyner AL (2000) Establishment and chimera analysis of 129/SvEv- and C57BL/6-derived mouse embryonic stem cell lines. *Biotechniques* **29**: 1024–1028, 1030, 1032

Britos-Bray M, Friedman AD (1997) Core binding factor cannot synergistically activate the myeloperoxidase proximal enhancer in immature myeloid cells without c-Myb. *Mol Cell Biol* **17**: 5127–5135

Chen CJ, Deng Z, Kim AY, Blobel GA, Lieberman PM (2001) Stimulation of CREB binding protein nucleosomal histone acetyltransferase activity by a class of transcriptional activators. *Mol Cell Biol* **21**: 476–487

Choi CY, Kim YH, Kim YO, Park SJ, Kim EA, Riemenschneider W, Gajewski K, Schulz RA, Kim Y (2005) Phosphorylation by the DHIPK2 protein kinase modulates the corepressor activity of Groucho. *J Biol Chem* **280**: 21427–21436

Choi CY, Kim YH, Kwon HJ, Kim Y (1999) The homeodomain protein NK-3 recruits Groucho and a histone deacetylase complex to repress transcription. *J Biol Chem* **274**: 33194–33197

Cockerill PN, Osborne CS, Bert AG, Grotto RJ (1996) Regulation of GM-CSF gene transcription by core-binding factor. *Cell Growth Differ* **7**: 917–922

D'Orazi G, Cecchinelli B, Bruno T, Manni I, Higashimoto Y, Saito S, Gostissa M, Coen S, Marchetti A, Del Sal G, Piaggio G, Fanciulli M, Appella E, Soddu S (2002) Homeodomain-interacting protein kinase-2 phosphorylates p53 at Ser 46 and mediates apoptosis. *Nat Cell Biol* **4**: 11–19

Hofmann TG, Moller A, Sirma H, Zentgraf H, Taya Y, Droge W, Will H, Schmitz ML (2002) Regulation of p53 activity by its interaction with homeodomain-interacting protein kinase-2. *Nat Cell Biol* **4**: 1–10

Imai Y, Kurokawa M, Tanaka K, Friedman AD, Ogawa S, Mitani K, Yazaki Y, Hirai H (1998) TLE, the human homolog of groucho, interacts with AML1 and acts as a repressor of AML1-induced transactivation. *Biochem Biophys Res Commun* **252**: 582–589

Isono K, Nemoto K, Li Y, Takada Y, Suzuki R, Katsuki M, Nakagawara A, Koseki H (2006) Overlapping roles for homeodomain-interacting protein kinases hipk1 and hipk2 in the med-

iation of cell growth in response to morphogenetic and genotoxic signals. *Mol Cell Biol* **26:** 2758–2771

Jenuwein T, Allis CD (2001) Translating the histone code. *Science* **293:** 1074–1080

Kanei-Ishii C, Ninomiya-Tsuji J, Tanikawa J, Nomura T, Ishitani T, Kishida S, Kokura K, Kurahashi T, Ichikawa-Iwata E, Kim Y, Matsumoto K, Ishii S (2004) Wnt-1 signal induces phosphorylation and degradation of c-Myb protein via TAK1, HIPK2, and NLK. *Genes Dev* **18:** 816–829

Kasper LH, Boussouar F, Ney PA, Jackson CW, Rehg J, van Deursen JM, Brindle PK (2002) A transcription-factor-binding surface of coactivator p300 is required for haematopoiesis. *Nature* **419:** 738–743

Katsumoto T, Aikawa Y, Iwama A, Ueda S, Ichikawa H, Ochiya T, Kitabayashi I (2006) MOZ is essential for maintenance of hematopoietic stem cells. *Genes Dev* **20:** 1321–1330

Kim WY, Sieweke M, Ogawa E, Wee HJ, Englmeier U, Graf T, Ito Y (1999) Mutual activation of Ets-1 and AML1 DNA binding by direct interaction of their autoinhibitory domains. *EMBO J* **18:** 1609–1620

Kim YH, Choi CY, Lee SJ, Conti MA, Kim Y (1998) Homeodomain-interacting protein kinases, a novel family of co-repressors for homeodomain transcription factors. *J Biol Chem* **273:** 25875–25879

Kitabayashi I, Aikawa Y, Nguyen LA, Yokoyama A, Ohki M (2001) Activation of AML1-mediated transcription by MOZ and inhibition by the MOZ-CBP fusion protein. *EMBO J* **20:** 7184–7196

Kitabayashi I, Eckner R, Arany Z, Chiu R, Gachelin G, Livingston DM, Yokoyama KK (1995) Phosphorylation of the adenovirus E1A-associated 300 kDa protein in response to retinoic acid and E1A during the differentiation of F9 cells. *EMBO J* **14:** 3496–3509

Kitabayashi I, Ida K, Morohoshi F, Yokoyama A, Mitsuhashi N, Shimizu K, Nomura N, Hayashi Y, Ohki M (1998a) The AML1-MTG8 leukemic fusion protein forms a complex with a novel member of the MTG8(ETO/CDR) family, MTGR1. *Mol Cell Biol* **18:** 846–858

Kitabayashi I, Yokoyama A, Shimizu K, Ohki M (1998b) Interaction and functional cooperation of the leukemia-associated factors AML1 and p300 in myeloid cell differentiation. *EMBO J* **17:** 2994–3004

Kondo S, Lu Y, Debbas M, Lin AW, Sarosi I, Itie A, Wakeham A, Tuan J, Saris C, Elliott G, Ma W, Benchimol S, Lowe SW, Mak TW, Thukral SK (2003) Characterization of cells and gene-targeted mice deficient for the p53-binding kinase homeodomain-interacting protein kinase 1 (HIPK1). *Proc Natl Acad Sci USA* **100:** 5431–5436

Kovacs KA, Steinmann M, Magistretti PJ, Halfon O, Cardinaux JR (2003) CCAAT/enhancer-binding protein family members recruit the coactivator CREB-binding protein and trigger its phosphorylation. *J Biol Chem* **278:** 36959–36965

Legube G, Trouche D (2003) Regulating histone acetyltransferases and deacetylases. *EMBO Rep* **4:** 944–947

Levanon D, Goldstein RE, Bernstein Y, Tang H, Goldenberg D, Stifani S, Paroush Z, Groner Y (1998) Transcriptional repression by AML1 and LEF-1 is mediated by the TLE/Groucho corepressors. *Proc Natl Acad Sci USA* **95:** 11590–11595

Li QJ, Yang SH, Maeda Y, Sladek FM, Sharrocks AD, Martins-Green M (2003) MAP kinase phosphorylation-dependent activation of Elk-1 leads to activation of the co-activator p300. *EMBO J* **22:** 281–291

Look AT (1997) Oncogenic transcription factors in the human acute leukemias. *Science* **278:** 1059–1064

Marmorstein R, Roth SY (2001) Histone acetyltransferases: function, structure, and catalysis. *Curr Opin Genet Dev* **11:** 155–161

Meyers S, Downing JR, Hiebert SW (1993) Identification of AML-1 and the (8;21) translocation protein (AML-1/ETO) as sequence-specific DNA-binding proteins: the runt homology domain is required for DNA binding and protein-protein interactions. *Mol Cell Biol* **13:** 6336–6345

Nguyen LA, Pandolfi PP, Aikawa Y, Tagata Y, Ohki M, Kitabayashi I (2005) Physical and functional link of the leukemia-associated factors AML1 and PML. *Blood* **105:** 292–300

Niki M, Okada H, Takano H, Kuno J, Tani K, Hibino H, Asano S, Ito Y, Satake M, Noda T (1997) Hematopoiesis in the fetal liver is impaired by targeted mutagenesis of a gene encoding a non-DNA binding subunit of the transcription factor, polyomavirus enhancer binding protein 2/core binding factor. *Proc Natl Acad Sci USA* **94:** 5697–5702

Ogawa E, Inuzuka M, Maruyama M, Satake M, Naito-Fujimoto M, Ito Y, Shigesada K (1993) Molecular cloning and characterization of PEBP2 beta, the heterodimeric partner of a novel *Drosophila* runt-related DNA binding protein PEBP2 alpha. *Virology* **194:** 314–331

Oike Y, Takakura N, Hata A, Kaname T, Akizuki M, Yamaguchi Y, Yasue H, Araki K, Yamamura K, Suda T (1999) Mice homozygous for a truncated form of CREB-binding protein exhibit defects in hematopoiesis and vasculo-angiogenesis. *Blood* **93:** 2771–2779

Okada H, Watanabe T, Niki M, Takano H, Chiba N, Yanai N, Tani K, Hibino H, Asano S, Mucenski ML, Ito Y, Noda T, Satake M (1998) AML1(−/−) embryos do not express certain hematopoiesis-related gene transcripts including those of the PU.1 gene. *Oncogene* **17:** 2287–2293

Okuda T, van Deursen J, Hiebert SW, Grosveld G, Downing JR (1996) AML1, the target of multiple chromosomal translocations in human leukemia, is essential for normal fetal liver hematopoiesis. *Cell* **84:** 321–330

Petrovick MS, Hiebert SW, Friedman AD, Hetherington CJ, Tenen DG, Zhang DE (1998) Multiple functional domains of AML1: PU.1 and C/EBPalpha synergize with different regions of AML1. *Mol Cell Biol* **18:** 3915–3925

Rebel VI, Kung AL, Tanner EA, Yang H, Bronson RT, Livingston DM (2002) Distinct roles for CREB-binding protein and p300 in hematopoietic stem cell self-renewal. *Proc Natl Acad Sci USA* **99:** 14789–14794

Sasaki K, Yagi H, Bronson RT, Tominaga K, Matsunashi T, Deguchi K, Tani Y, Kishimoto T, Komori T (1996) Absence of fetal liver hematopoiesis in mice deficient in transcriptional coactivator core binding factor beta. *Proc Natl Acad Sci USA* **93:** 12359–12363

Schwartz C, Beck K, Mink S, Schmolke M, Budde B, Wenning D, Klempnauer KH (2003) Recruitment of p300 by C/EBPbeta triggers phosphorylation of p300 and modulates coactivator activity. *EMBO J* **22:** 882–892

Soutoglou E, Viollet B, Vaxillaire M, Yaniv M, Pontoglio M, Talianidis I (2001) Transcription factor-dependent regulation of CBP and P/CAF histone acetyltransferase activity. *EMBO J* **20:** 1984–1992

Takakura N, Watanabe T, Suenobu S, Yamada Y, Noda T, Ito Y, Satake M, Suda T (2000) A role for hematopoietic stem cells in promoting angiogenesis. *Cell* **102:** 199–209

Tanaka T, Kurokawa M, Ueki K, Tanaka K, Imai Y, Mitani K, Okazaki K, Sagata N, Yazaki Y, Shibata Y, Kadowaki T, Hirai H (1996) The extracellular signal-regulated kinase pathway phosphorylates AML1, an acute myeloid leukemia gene product, and potentially regulates its transactivation ability. *Mol Cell Biol* **16:** 3967–3979

Tanaka Y, Naruse I, Hongo T, Xu M, Nakahata T, Maekawa T, Ishii S (2000) Extensive brain hemorrhage and embryonic lethality in a mouse null mutant of CREB-binding protein. *Mech Dev* **95:** 133–145

Thiagalingam S, Cheng KH, Lee HJ, Mineva N, Thiagalingam A, Ponte JF (2003) Histone deacetylases: unique players in shaping the epigenetic histone code. *Ann NY Acad Sci* **983:** 84–100

Wang Q, Stacy T, Binder M, Marin-Padilla M, Sharpe AH, Speck NA (1996a) Disruption of the Cbfa2 gene causes necrosis and hemorrhaging in the central nervous system and blocks definitive hematopoiesis. *Proc Natl Acad Sci USA* **93:** 3444–3449

Wang Q, Stacy T, Miller JD, Lewis AF, Gu TL, Huang X, Bushweller JH, Bories JC, Alt FW, Ryan G, Liu PP, Wynshaw-Boris A, Binder M, Marin-Padilla M, Sharpe AH, Speck NA (1996b) The CBFbeta subunit is essential for CBFalpha2 (AML1) function *in vivo*. *Cell* **87:** 697–708

Wiggins AK, Wei G, Doxakis E, Wong C, Tang AA, Zang K, Luo EJ, Neve RL, Reichardt LF, Huang EJ (2004) Interaction of Brn3a and HIPK2 mediates transcriptional repression of sensory neuron survival. *J Cell Biol* **167:** 257–267

Yao TP, Oh SP, Fuchs M, Zhou ND, Ch'ng LE, Newsome D, Bronson RT, Li E, Livingston DM, Eckner R (1998) Gene dosage-dependent embryonic development and proliferation defects in mice lacking the transcriptional integrator p300. *Cell* **93:** 361–372

Zhang DE, Hetherington CJ, Meyers S, Rhoades KL, Larson CJ, Chen HM, Hiebert SW, Tenen DG (1996) CCAAT enhancer-binding protein (C/EBP) and AML1 (CBF alpha2) synergistically activate the macrophage colony-stimulating factor receptor promoter. *Mol Cell Biol* **16:** 1231–1240

Zhang Q, Yoshimatsu Y, Hildebrand J, Frisch SM, Goodman RH (2003) Homeodomain interacting protein kinase 2 promotes apoptosis by downregulating the transcriptional corepressor CtBP. *Cell* **115:** 177–186